CATALYTIC STUDIES OF SUPPORTED Pd-Au CATALYSTS

A Thesis

by

PRAVEENKUMAR BOOPALACHANDRAN

Submitted to the Office of Graduate Studies of
Texas A&M University
in partial fulfillment of the requirements for the degree of

MASTER OF SCIENCE

May 2006

Major Subject: Chemistry

CATALYTIC STUDIES OF SUPPORTED Pd-Au CATALYSTS

A Thesis

by

PRAVEENKUMAR BOOPALACHANDRAN

Submitted to the Office of Graduate Studies of
Texas A&M University
in partial fulfillment of the requirements for the degree of

MASTER OF SCIENCE

Approved by:

Chair of Committee,   D. Wayne Goodman
Committee Members, Michael P. Rosynek
                               Raymond E. Schaak
                               Daniel F. Shantz
Head of Department, Emile A. Schweikert

May 2006

Major Subject: Chemistry

ABSTRACT

Catalytic Studies of Supported Pd-Au Catalysts. (May 2006)

Praveenkumar Boopalachandran, B.Tech., University of Madras;

M.S., Texas A&M University – Commerce

Chair of Advisory Committee: Dr. D. Wayne Goodman

Although Pd-Au high-surface area catalysts are used in industry to improve activity and selectivity, a thorough understanding of the nature of these enhancements is lacking. A molecular-level understanding of catalytic reactions under actual reaction conditions is the ultimate goal. This thesis is mainly focused on the application of Pd-Au supported catalysts for vinyl acetate synthesis and CO oxidation reactions using high-surface area catalysts. We have attempted to improve the conventional Pd-Au based catalyst by synthesizing novel acetate-based and polymer-based catalysts. The corresponding catalytic reactivity and selectivity were measured and compared to conventional Pd-Au based catalyst systems. Subsequent characterization was performed using characterization techniques, such as, X-ray diffraction (XRD) and transmission electron microscopy (TEM).

From our bimetallic catalytic studies, it was evident that the addition of Au to Pd leads to increased reactivity and selectivity. This surface modification is an important factor in the altered reaction kinetics for vinyl acetate (VA) synthesis and CO oxidation reactions. Promoted and unpromoted Pd-Au/SiO_2/K^+ catalyst were used for VA synthesis and the effect of pre-adsorbed O_2, acetic acid and the role of oxygen were explored.

The VA reaction rate of novel acetate-based Pd-Au/SiO$_2$ catalyst was 3.5 times higher than conventional Pd-Au catalysts. Also, 100% selectivity was obtained for acetate-based Pd-Au/SiO$_2$ at 130 ^{o}C and the VA formation rate was comparable to that of conventional Pd-Au catalysts. Therefore, the acetate-based Pd-Au/SiO$_2$ catalyst seems very promising and can be explored further. Also, Pd(1):Au(4)/SiO$_2$ catalysts demonstrate 100% CO conversion at much lower temperatures (90 ^{o}C) compared with other Pd-Au based catalysts. Furthermore, we were successful in obtaining sufficient CO oxidation activity with increased metal loading (5 wt%) and these catalysts did not deactivate under above-ambient reaction temperature conditions, which make 1:4 Pd-Au/SiO$_2$ catalyst a good candidate for further exploration in CO oxidation reactions.

ACKNOWLEDGEMENTS

It is a pleasure to thank many people who made this thesis possible. I thank Dr.Wayne Goodman, my research advisor, for his continuous guidance, inspiration and enthusiasm. He manages to strike the perfect balance between providing direction and encouraging independence. I also like to thank the other committee members: Dr. Raymond E. Schaak, Dr. Michael P. Rosynek and Dr. Daniel F. Shantz for their advice. I deeply appreciate Julie Wilson and Mrs. Amy Liu for their kindness during the time of this research. I would like to thank Dheeraj Kumar and Dr. Mingshu Chen for their collaboration, friendship and help with solving numerous problems that I have encountered in/out of the laboratory. Also, thanks to Rob Cable for synthesizing acetate-based catalysts. I am grateful to many people in the Department of Chemistry who have assisted me in the course of this work. I am forever indebted to my parents for their understanding, endless patience and encouragement when it was required. Finally, I thank God for giving me the confidence and the blessings during this research.

TABLE OF CONTENTS

LIST OF FIGURES

FIGURE   Page

FIGURE   Page

INTRODUCTION

Catalysis finds application in various fields, such as fuel cells, oil refining, chemical processing, exhaust systems, etc. The fundamental concept of heterogeneous catalysis is that the catalytic substance has a prominent catalytic activity at the surface which is termed as the active site of the catalyst [1, 2]. Typically most industrial catalysts are nanometer-scale metal particles with many active centers supported on inert, porous metal oxide substrates [2]. Metal oxides such as silica, alumina and magnesia are the most widely used supports [1, 2]. The main purpose of the support is to disperse and stabilize the active centers, while the support itself usually is catalytically inactive [2]. These supported catalysts are often referred to as high-surface area catalysts.

A catalyst cannot change the ultimate equilibrium determined by thermodynamics but it can change the kinetics of the chemical reaction [1, 2, 3]. The preparation methods, the composition of the active metals and the conditions employed govern the behavior of the catalysts which is described in global terms of activity, selectivity and deactivation. Activity is expressed in units of amount of product made in the reactor per unit time and per unit of reactor volume [2]. The selectivity is a measure of the extent to which it accelerates the reaction to form one or more of the desired products that are usually intermediates, instead of those formed by reaction to the overall state of lowest free energy [1, 2]. Activity and selectivity usually varies with pressure, temperature, reactant composition, extent of conversion, as well as, with the nature of the catalyst [2]. On the other hand, a catalyst may deactivate for a wide variety of factors such as poisoning,

———————————————————————

This thesis follows the style used in Surface Science.

fouling and sintering [1, 2]. The best performance of a heterogeneous catalyst is achieved by varying the preparation procedures, the operating conditions and the catalysts constituents. The catalyst constituents vary from monometallic to multi metallic systems, and typically contain promoters, poisons, etc. Bimetallic supported catalysts have attracted major attention because of their enhanced catalytic activity and selectivity compared to monometallic supported catalysts [3, 4, 5, 6].

Bimetallic Supported Catalysts

Bimetallic catalysts have many applications in the areas of corrosion science, catalysis and electrochemistry [1, 2]. Research efforts are concentrated in understanding correlations of catalytic activity and selectivity with electronic, structural, and physicochemical properties of these catalyst systems. Understanding the enhancement of activities and/or selectivities of bimetallic catalysts remains a significant research challenge.

Ensemble Effect and Ligand Effect

The changes in the physical and chemical properties of the catalysts due to the addition of a second metal component is usually discussed in terms of "ensemble effects" and "ligand effects". The "ensemble effect" refers to the factors where certain number of atoms in a particular geometry are required to facilitate a particular catalytic process [7]. On the other hand, "ligand effects" describes the modification resulting from the addition of one metal to a second metal leading to the formation of heteronuclear metal-metal

bonds involving charge transfer between the metals [7]. These theories are well accepted to explain the catalytic activity and selectivity in supported bimetallic catalyst systems.

Pd-Au Bimetallic Supported Catalysts

Palladium (Pd) is a well known catalyst for many reactions which are of industrial and environmental importance [7]. A major drawback of using Pd-only catalysts is the formation of carbides, i.e. PdC_x, as shown in the Fig. 1 [8]. In case of vinyl acetate synthesis [8] using Pd(1 wt%)/SiO$_2$ and Pd(5 wt%)/SiO$_2$ the reaction rate dropped to 35% and 50% of its initial rate, respectively [8]. It was seen that the interstitial carbon in Pd may significantly alter the bulk and surface structure of Pd and can lead to catalytic deactivation in reactions involving hydrocarbons.

On the other hand, Au catalysts although traditionally considered inert, have received great attention due to the surprisingly high catalytic activity exhibited in CO oxidation and epoxidation of propylene reactions [7, 9, 10]. An important requisite in achieving good catalytic activity using gold is the nanoscale synthesis of supported gold by various complicated preparation techniques. Many studies reveal that the addition of gold to palladium catalysts has pronounced catalytic effect [3, 6]. It is plausible that the electronic and geometric properties are tuned by the addition of Au with highly optimized sites [3, 6, 11]. Also, model catalytic studies have shown that Pd and Au are completely miscible as solid solutions and that there is only a 4% lattice mismatch between Pd(111) and Au(111) [7].
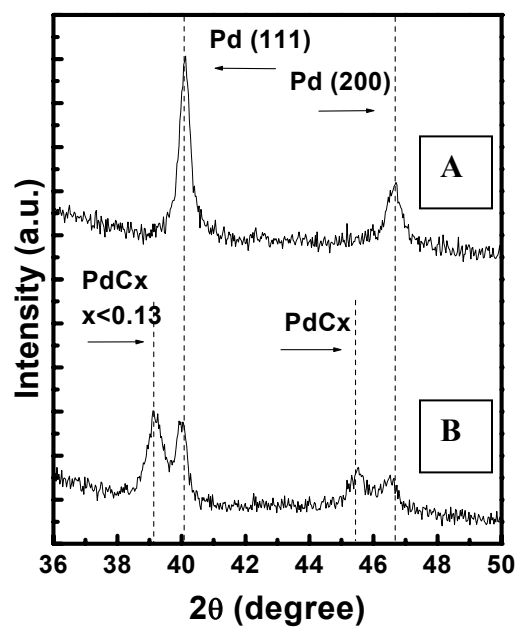
Fig. 1.   XRD data for Pd/SiO$_2$ catalyst; A) freshly reduced; B) after VA reaction (Ref. [8]).

Surface composition is a key element in understanding the role of alloying in Pd-Au bimetallic catalysts [11, 12]. The surface properties of heterogeneous catalysts show numerous unique properties that are significantly different than the bulk catalyst structure. Model catalytic studies have shown that the surface concentration of Pd-Au alloy differs from the corresponding bulk concentration [7, 13, 14, 15]. Fig. 2 [7] shows the phase diagram of surface versus bulk plotted as a function of Pd-Au ratio. The studies were carried out using Pd-Au alloys on Mo(110) and the surface concentrations were measured using low energy ion scattering spectroscopy (LEISS) [7]. It was observed that the surface concentration of Au ranges from 40% to 96% while the bulk concentration of Au varies from 10% to 90%. This compositional variation in the concentration is generally attributed to the difference in surface free energies between Pd and Au [7, 13]. The surface free energy of palladium is 2.043 J/m^2, which is higher than the surface free energy of gold (1.626 J/m^2) [7]. In order to minimize the surface free energy, gold segregates to the surface. These results suggest that the surface composition can be controlled by altering Pd-Au concentration.

Therefore, it is possible to synthesize Pd-Au supported catalysts with controlled surface ratio by altering the bulk metal ratio, and potentially leading to a better understanding of the relationships between catalytic activity/selectivity, and surface structure. This is particularly relevant to vinyl acetate synthesis using supported Pd-Au catalysts.
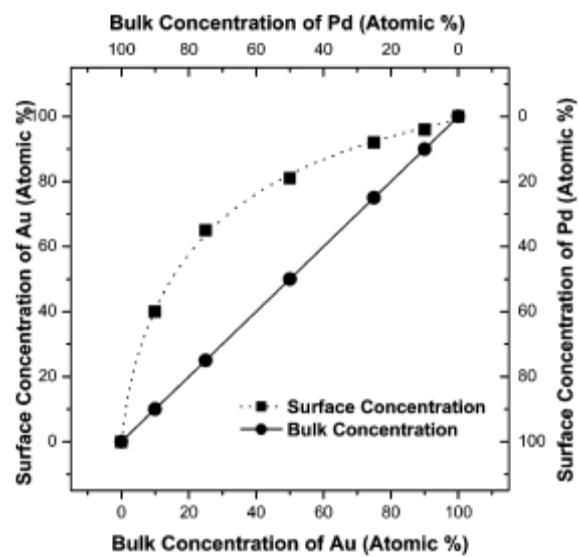
Fig. 2. Surface concentration of various Pd-Au alloys on Mo(110) measured by LEISS compared to the bulk concentration (Ref. [7]).

Vinyl Acetate (VA) Synthesis

VA was first produced in 1912 as a by product in the synthesis of ethylidene diacetate. VA is an important monomer for the synthesis of polyvinyl alcohol and polyvinyl acetate, and is also used in the production of paints [2]. Two commercial processes for the VA synthesis are a liquid process with a homogeneous palladium-containing catalyst ($PdCl_2$ and $CuCl_2$) and a vapor phase process with a heterogeneous palladium-containing catalyst [16]. The liquid phase process was converted to a vapor phase process, which accounts for more than 75% of the currently available capacity of VA production. The annual production of VA in USA is about 3.65 billion pounds [2]. The conventional vapor phase process involves passing 4:1 acetylene-to-acetic acid mixture over a catalyst bed made of zinc acetate-saturated activated carbon between 180 ^{o}C-200 ^{o}C [17, 18]. Another commercial manufacturing process of vinyl acetate involves the reaction between acetaldehyde and acetic anhydride. Furthermore, VA can also be synthesized by reacting vinyl chloride with sodium acetate in solution at 50 ^{o}C-75 ^{o}C [17, 18]. Currently, the synthesis of VA is carried out via the gas phase acetoxylation of ethylene over various palladium-based catalysts as the vapor phase addition of acetic acid to acetylene on a Zn/C catalyst is more expensive [19].

The ideal reaction pathway is given by [19, 20, 21, 22]

$$C_2H_4 + CH_3COOH + 1/2O_2 \rightarrow C_2H_3OOCCH_3 + H_2O \tag{1}$$

Possible side reactions are given by

$$C_2H_4(C_xH_y) + O_2 \rightarrow CO_2(CO) + H_2O \tag{2}$$

$$CH_3COOH + O_2 \rightarrow CO_2(CO) + H_2O \tag{3}$$

$$C_2H_3OOCH_3 \rightarrow CO_2(CO) + H_2O \tag{4}$$

From equations (2)-(4), it is evident that VA selectivity is a key issue for the gas phase acetoxylation of ethylene reaction. It was observed that the activation energy obtained for the reaction of ethylene with oxygen for CO_2 formation was almost identical in the presence and in the absence of acetic acid suggesting that CO_2 is mainly derived from ethylene [3, 6]. Furthermore, the selectivity of vinyl acetate formation increases with an increase in the ratio of acetic acid to ethylene [3, 6].

Studying the reaction kinetics between monometallic and bimetallic catalyst systems can lead to the understanding of the catalytic activity and selectivity. The kinetics of VA using model catalytic systems such as Pd(100) catalyst have been shown to be comparable to the results obtained using supported Pd catalysts [6]. Based on these results, it is assumed that the structure of the active sites on a silica supported Pd and Pd-Au alloy clusters is similar to that of silica supported Pd and Pd-Au high surface area catalysts.

In a model catalytic study, to probe the surface structure of the Pd-Au alloy clusters as well as their catalytic reactivity, a TPD study of deuterated ethylene (C_2D_4) adsorption and dehydrogenation on the silica-supported Pd and Pd-Au alloy clusters was carried out [23]. 2.0 L of C_2D_4 was dosed on 1.0 ML Pd/SiO_2, 0.2 ML Au/1.0 ML Pd/SiO_2 and 1.0 ML Au/1.0 ML Pd/SiO_2 surface at 90 K. Fig. 3 [23] shows a broad feature with a desorption temperature peak maximum at 250 K, assigned to contributions from π-bonded and di-σ bonded C_2D_4. With 0.2 ML Au deposition to 1.0 ML Pd/SiO_2 clusters and annealing, a significant loss of C_2D_4 desorption intensity was observed. Furthermore, with 1.0 ML Au deposition to 1.0 ML Pd/SiO_2 clusters and annealing, a significant further loss of C_2D_4 desorption intensity was observed with the desorption
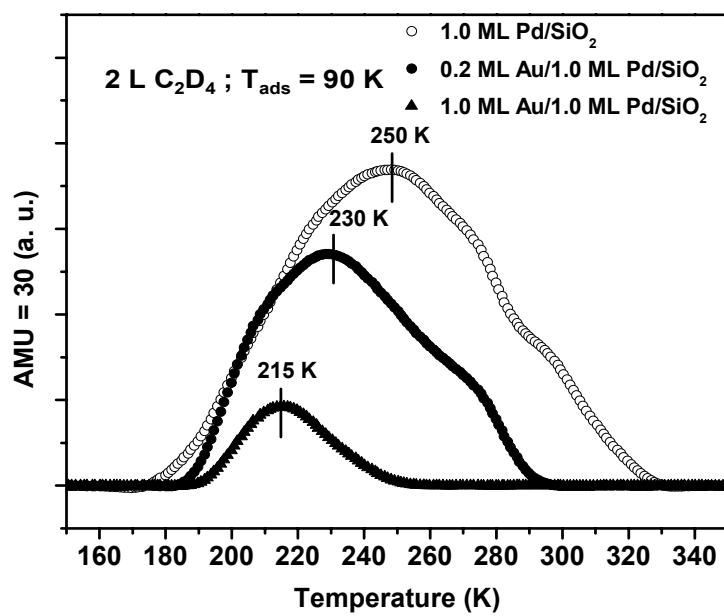
Fig. 3.   TPD of C_2D_4 with 2.0 L C_2D_4 exposure at 90 K on 1.0 ML Pd/SiO$_2$,
0.2 MLAu/1.0 ML Pd/SiO$_2$; and 1.0 ML Au/1.0 ML Pd/SiO$_2$ (Ref. [23]).

peak maximum shift to 215 K. These results indicate that ethylene binds less strongly on Pd-Au cluster surface compared to Pd cluster surface. The addition of Au to Pd clusters leads to attenuation of the stronger di-σ bonded C_2D_4 which may further decompose into carbon species on the surface thus blocking and poisoning the surface active sites [20, 21, 22, 23, 24, 25, 26].

In another study, CO was used as a probe molecule to characterize the surface adsorption sites [23]. 1.0 L of CO was dosed on bare silica, 1.0 ML Pd/SiO_2, 1.0 ML Au/SiO_2, 1.0 ML Pd/1.0 ML Au/SiO_2 and 1.0 ML Au/1.0 ML Pd/SiO_2 surface at 90 K and annealed to 800 K. Fig. 4 [23], in a TPD study of CO on bare SiO_2, a broad feature centered at 135 K was observed from CO adsorbed on the SiO_2 support. For CO TPD on 1.0 ML Pd/SiO_2, additional features centered at 465, 320, and 250 K were observed. The feature at 465 K is assigned to CO adsorbed on Pd three-fold hollow sites; features at 250 and 320 K are assigned to CO adsorbed on atop Pd sites, and the desorption feature between 320 and 465 K are assigned to CO on Pd bridging site. With 1.0 ML Pd deposition to 1.0 ML Au/SiO_2 clusters and annealing, a significant loss of CO desorption intensity was observed. Furthermore, with 1.0 ML Au deposition to 1.0 ML Pd/SiO_2 clusters and annealing, a significant loss of CO desorption intensity was observed. As CO is a by-product in VA synthesis reaction, the strong adsorption of CO on Pd may poison the active surface site. The addition of Au to Pd clusters leads to attenuation of the strong adsorption of CO on Pd sites thus increasing the reactivity.
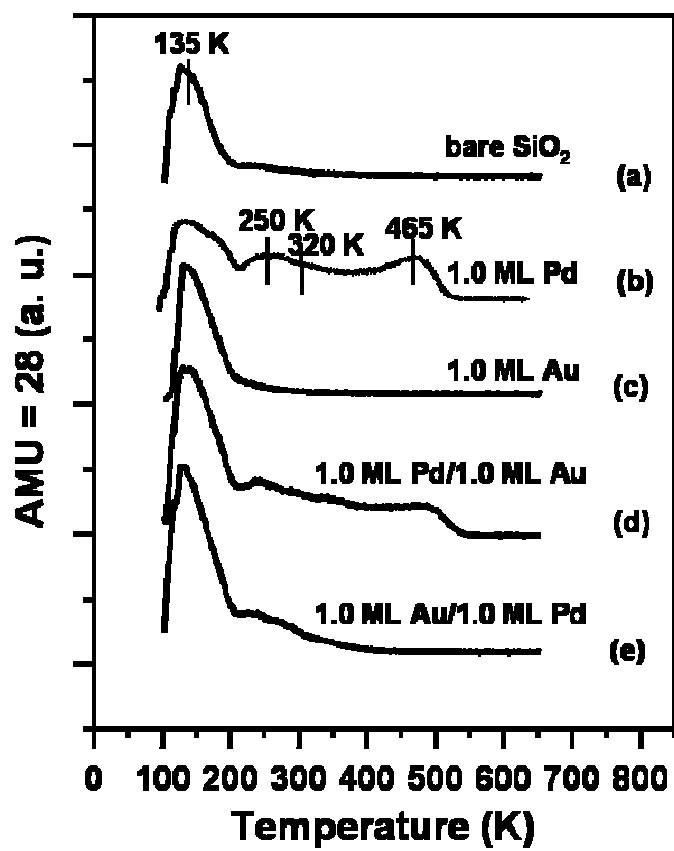
Fig. 4.   TPD spectra of CO: (a) with 1.0 L exposure at 90 K on pure SiO_2; (b) 1.0 ML Pd/SiO_2; (c) 1.0 ML Au/SiO_2; 1.0 ML Pd/1.0 ML Au/SiO_2; and (e) 1.0 ML Au/1.0 ML Pd/SiO_2 (Ref. [23]).

Furthermore, to investigate the promotional effect of Au in a Pd-Au alloy catalyst, acetoxylation of ethylene to vinyl acetate was used as a probe reaction [27]. These experiments were carried out on Pd/Au(100) and Pd/Au(111) at 453 K. VA formation rises to a maximum rate as the Pd coverage is lowered to approximately 0.1 monolayer, then decreases sharply with a further decrease in the Pd coverage below 0.1 ML, as shown in Fig. 5[27] . It is evident that the VA formation rate for Pd/Au(100) are significantly higher than for Pd/Au(111) over the entire Pd coverage. The increased rate was attributed to the formation of Pd monomers in these catalyst systems. Furthermore, CO was used as a probe molecule on Pd/Au(100) and Pd/Au(111) surfaces at 100 K followed by an anneal, and the corresponding infrared absorption reflection spectroscopy (IRAS) were obtained as shown in Fig. 6[27] . Intense CO features between 1900 to 2000 cm-^{1} corresponding to CO adsorption on two-fold bridging and/or three-fold hollow sites were observed for multilayer Pd on Au(100) and Au(111). Upon annealing these catalysts to 600 K or higher, the CO features in the IRAS data corresponding to atop sites between 2125~2080 cm-^{1} increase significantly. These results demonstrate that continuous surface Pd ensembles are broken up upon annealing to form isolated Pd sites.
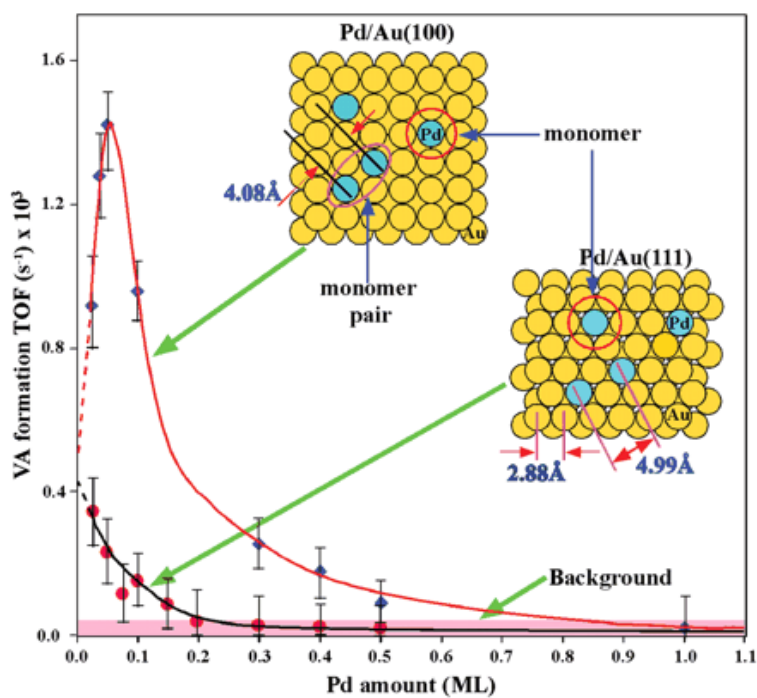
Fig. 5.   VA formation rates as a function of Pd coverage on Au (100) and Au (111) (Ref. [27]).
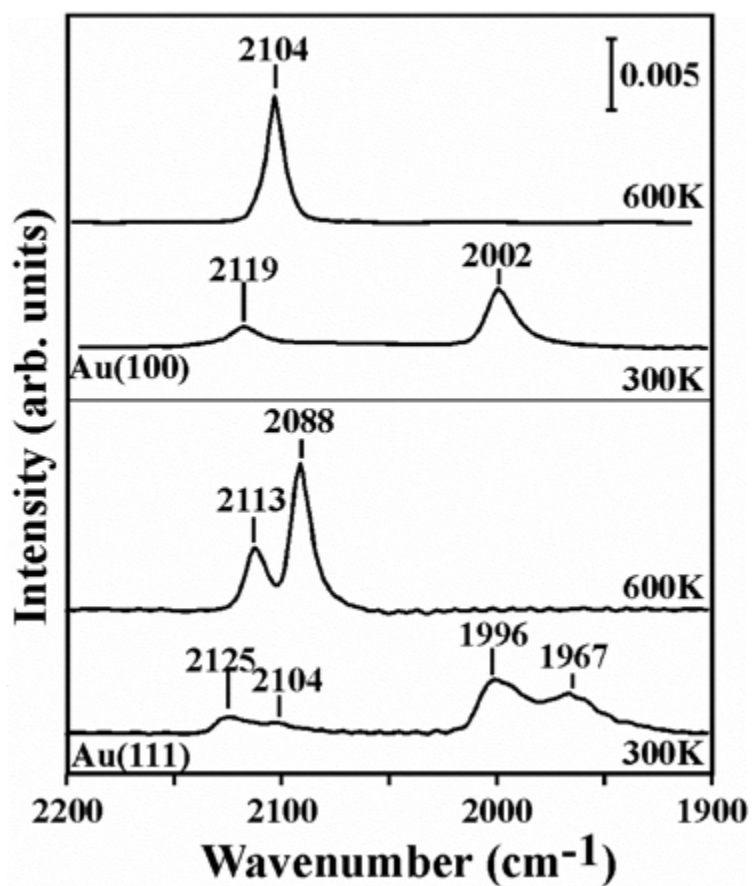
Fig. 6.   IRAS spectra for CO adsorption on Pd/Au(100) and Pd/Au(111) surface at 100 K showing the presence (300 K anneal) and absence (600 K anneal) of contiguous Pd sites. The Pd/Au(100) and Pd/Au(111) surface were prepared by depositing 4 ML of Pd at 100 K, then annealed to 300 K and 600 K, respectively (Ref. [27]).

Recently, Neurock and co-workers [20] used density functional theory (DFT) calculations to propose elementary steps representative of the vinyl acetate monomer synthesis. Seven elementary steps are suggested: oxygen addition (5), dissociative adsorption of acetic acid (6), ethylene adsorption (7), ethylene insertion (8), β-C-H bond scission (9), VAM desorption (10), and associative desorption of water (11)

$$1/2O_2 \ (g) \rightarrow O \ (a) \tag{5}$$

$$O \ (a) + CH_3COOH \ (g) \rightarrow \ CH_3COO \ (a) + OH \ (a) \tag{6}$$

$$CH_3COO \ (a) + OH \ (a) + C_2H_4 \ (g) \rightarrow CH_3COO \ (a) + OH \ (a) + C_2H_4 \ (g) \tag{7}$$

$$CH_3COO \ (a) + OH \ (a) + C_2H_4 \ (g) \rightarrow CH_3COO \ C_2H_4 \ (a) + OH \ (a) \tag{8}$$

$$CH_3COO \ C_2H_4 + OH \ (a) \rightarrow CH_3COO \ C_2H_3 \ (a) + OH \ (a) + H \ (a) \tag{9}$$

$$CH_3COO \ C_2H_3 \ (a) + OH \ (a) + H \ (a) \rightarrow CH_3COO \ C_2H_3 \ (g) + OH \ (a) + H \ (a) \tag{10}$$

$$OH \ (a) + H \ (a) \rightarrow H_2O \ (g) \tag{11}$$
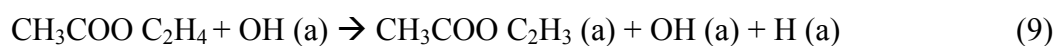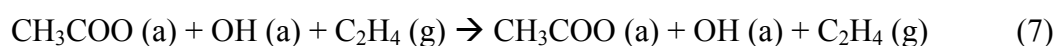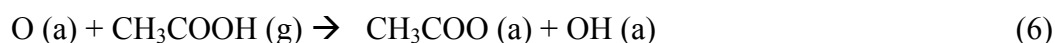
The overall energy diagram for each step of the cycle is shown in Fig. 7 [20]. These authors suggest that ethylene insertion and C-H bond activation are the most highly endothermic paths. C-H scission is much more favorable in the presence of adjacent oxygen species that readily accepts a proton; the presence of oxygen enhances the stability of the acetate species by 12 kJ/mol. These results are in good agreement with the experimental observations indicating the yield for the deprotonation of acetic acid to the adsorbed acetate can be increased significantly by enhancing the Bronsted basicity of the surface with chemisorbed oxygen [20].
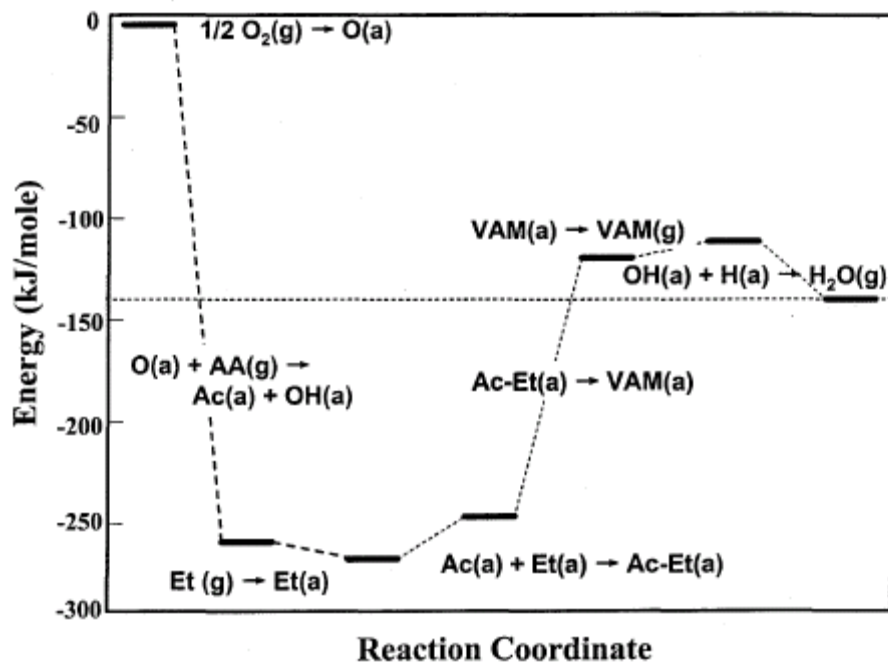
Fig. 7.   The overall energy diagram for vinyl acetate synthesis. VAM denotes vinyl acetatemonomer, Ac acetate, Et ethylene, AA acetic acid, (a) adsorbed species, and (g) gas phase species (adapted from Ref. [20]).

The reaction mechanism for VA synthesis remain uncertain, however two pathways have been proposed in the literature [12]: (i) adsorption and subsequent activation of ethylene to form vinyl acetate species that then couples with a coadsorbed acetate species to form VA; and (ii) adsorbed ethylene reacts with an adsorbed acetate nucleophile to form an ethyl-like-intermediate which then undergoes β-H elimination to form VA. Both mechanisms assume that the coupling of surface ethylene species and acetate to form VA is the rate-limiting step. Fig. 8 [27] shows the schematic representation of the coupling reaction between surface ethylene and acetate species facilitated by a Pd-monomer pair. based on the bond lengths of the parent reactant molecules, the optimum distance between two active sites to couple the reacting species is approximately 3.40 Å. The nearest spacing between two neighboring Pd monomers is 4.08 Å on the Pd/Au(100) alloy surface.
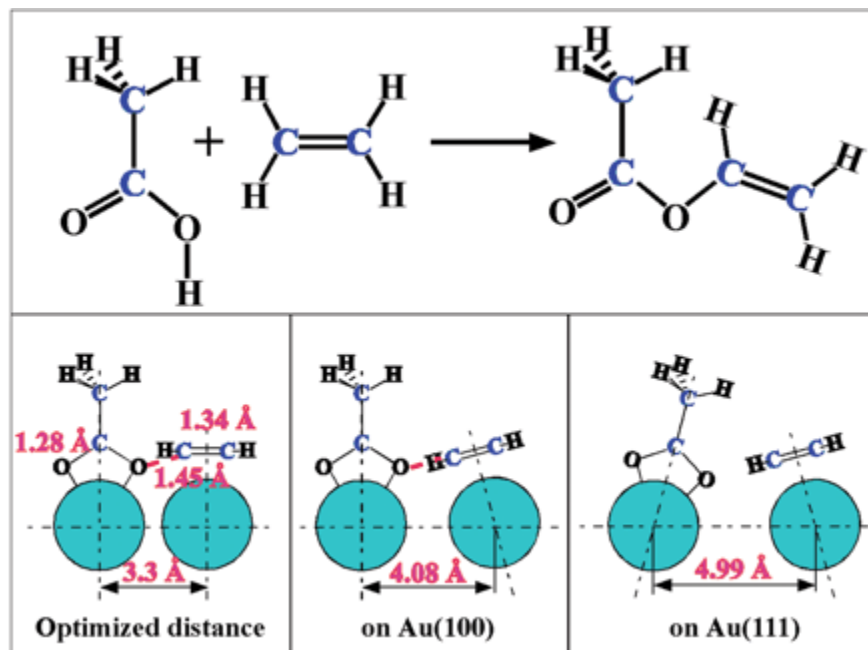
Fig. 8.   Schematic for VA synthesis from acetic acid and ethylene. The optimized distance between the two active centers for the coupling of surface ethylenic and acetate species to form VA is estimated to be 3.3 Å. With lateral displacement, coupling of an ethylenic and acetate species on a Pd monomer pair is possible on Au(100) but impossible on Au(111) (Ref. [27]).

This distance is acceptably close for coupling of the adsorbed surface species. On the other hand, on Pd/Au(111) alloy surface, the nearest distance between two neighboring Pd monomers is 4.99 Å, a distance much greater than the optimum distance, 3.40 Å. As a consequence, Pd/Au(100) alloy surface shows a much higher rate for VA synthesis than that of Pd/Au(111). Therefore, these results imply that larger Pd ensembles containing contiguous Pd atoms are indeed much less efficient than a properly spaced pair of Pd monomers.

The aim of the present study is to investigate the effect of the gold on palladium catalysts in the synthesis of VA by the gas phase acetoxylation of ethylene. The choice of Au as a second metal is dictated by its enhanced activity. By adopting wet impregnation technique, a series of silica supported Pd-Au catalysts with different Pd-Au ratios were synthesized. Also, we have made significant attempts to improve the Pd-Au based catalyst and compare the reaction rate and selectivity with the conventional catalysts.

CO Oxidation

The important applications for CO oxidation include fuel cells, gas sensing, chemical processing, exhaust systems for pollution control and air purification systems [28, 29, 30, 31, 32, 33, 34, 35, 36]. The CO oxidation reaction is

$$CO+1/2O_2 \rightarrow CO_2 \tag{12}$$

It is well known that gold is the least reactive metal and has been regarded as inactive as a heterogeneous catalyst [9, 28, 29, 30]. The low chemical activity of gold is due to the filled 5d shell and relatively high value of first ionization potential, with the result that gold catalysts has poor chemisorption properties [31]. However, when gold is deposited as ultra-fine particles on metal oxide supports, its catalytic activity increases drastically [32]. The interest in the use of gold in heterogeneous catalysis has recently increased on the basis of experimental evidences of its surprisingly high activity in the low temperature oxidation of CO [4]. These results contrast earlier studies showing that gold surfaces were inactive towards adsorption of O_2 gas at 300 K [4]. In this aspect, the support plays a major role in the catalytic behavior of this metal.

The catalyst supported on active oxides exhibit superior activity and is attributed to their ability to donate reactive oxygen. Most likely oxide vacancies are formed near to the gold-support interface offering a new site for oxygen adsorption [4]. These sites are abundant in the proximity of the gold particles due to the Schottky junction between gold and the n-type semiconducting oxides [4]. Therefore, these sites along the perimeter of gold-support interface would be favored for the reaction between CO adsorbed on Au and the oxygen adsorbed on the support. For these classes of supported catalysts, the

dependence of the activity on the gold particle size is not critical. However, the pre-treatment conditions of the catalysts have great influence on the final activity.

On the other hand, gold catalysts supported on inert oxide supports need to be prepared in a highly dispersed state. For these systems, oxygen activation is expected to occur directly on the gold particles [4]. An enhanced activity may rise from the geometric effects associated with defect sites such as kinks, steps and edges, or from electronic effects arisen from the variations in the density of states of small gold particles.

To synthesize highly dispersed gold catalysts; various methods have been used, including deposition-precipitation, coprecipitation and chemical vapor deposition [9, 34]. Conventional impregnation methods were considered to be ineffective as the particle size of gold was larger than 30 nm, a size shown to be inactive for CO oxidation [9, 33, 34, 35, 36]. The major problem encountered in using highly dispersed gold for CO oxidation is the marked dependence of the activity on the gold particle size [32, 36]. Precise cluster size distributions are of great importance for the reactivity of such supported clusters [30]. Furthermore, nano-gold particles have the tendency to deactivate under above-ambient reaction temperature conditions [36]. The reason for this failure is the sensitivity of the catalyst surface to pre-treatment and to reaction conditions. The use of bimetallic catalysts can be a way to limit such dependence, by increasing the resistance to particle sintering. Furthermore, recent studies have shown superior activities of supported alloyed Pd-Au catalysts in different types of reaction such as in the hydrodechlorination of chlorofluorocarbons (CFCs), in the hydrodesulphurization reaction and in the direct peroxide formation from H_2-O_2 mixtures.

CO oxidation is purported to occur exclusively on Pd in a Pd-rich alloy surface in Pd-Au catalysts since Au/SiO_2 shows no reactivity [35]. In a study of electrochemical oxidation of CO, it has been suggested that CO oxidation occurs on Pd-Au alloy surface by the following steps [6, 37]

$$Pd + CO \rightarrow Pd\text{-}CO \tag{13}$$

$$Pd + O \rightarrow Pd\text{-}O \tag{14}$$

$$Pd\text{-}O + Au \rightarrow Pd + Au\text{-}O \tag{15}$$

$$Pd\text{-}O + Pd\text{-}CO \rightarrow 2Pd + CO_2 \tag{16}$$

$$Au\text{-}O + Pd\text{-}CO \rightarrow Au + Pd + CO_2 \tag{17}$$

From equations (13)-(17), it is evident that the migration of O_{ad} from Pd to Au is an important step in this reaction, which accounts for higher CO conversion compared to Au/SiO_2.

The aim of the present study is to investigate the effect of the palladium on gold catalysts in the oxidation of CO by O_2. The choice of Pd as a second metal is dictated by its well recognized activity in this type of reaction. Using a wet impregnation technique, a series of silica supported Pd-Au catalysts with different Pd-Au ratios were synthesized. Silica was used as a support because of its inert character, allowing us to investigate the reciprocal effects of the two metals without the interference from metal-support interaction. Also, we have made significant attempts to improve the Pd-Au based catalyst and compare CO conversion as a function of temperature with conventional catalysts.

EXPERIMENTAL

Catalyst Preparation

Some of the common methods employed to synthesize supported catalysts include incipient wetness method, ion exchange, spreading and wetting and deposition-precipitation method [2]. In our current study, incipient wetness method was used to synthesize supported Pd(1.0 wt%)-Au(0.5 wt%)/SiO_2 and Pd(1.0 wt%)-Au(0.5 wt%)-K(2.5 wt%)/SiO_2 catalysts. As shown in Fig. 9 high surface area SiO_2 (Aldrich No. 7631-86-9) with a surface area of 600 m^2/gm, a particle size of 230-400 mesh, and a pore volume of 1.1 ml/g was used as a catalyst support. A Pd^{2+} solution and Au solution was prepared by dissolving $Pd(NO_3)_2$ and $HAuCl_4$ (C.P., commercial source) into demonized water. The precursor solutions were then added to equal volume of SiO_2 support for the synthesis of Pd-Au/SiO_2 catalyst. In addition, potassium acetate solution was added to the precursor impregnated support for the synthesis of Pd-Au/SiO_2/K^+ catalyst. $Na_2SiO_3.9H_2O$ was added rapidly to these impregnated catalysts and was allowed to dry for 4 hours in a covered beaker. The precursor was dried extensively under vacuum at 393 K prior to use. The procedure for the incipient wetness method is described in detail elsewhere [38].

On the other hand, to synthesize acetate based Pd-Au/SiO_2, Pd^{2+} solution was dissolved in tetraethyleneglycol (TEG), 0.1M in HCl, by stirring. Then $HAuCl_4*3H_2O$ was added in the correct stoichiometric ratio. The solution was stirred under Ar for ~1 hour, and then a solution of sodium acetate in TEG was added dropwise while stirring under Ar. The solution was heated to reflux for 1.5 hr, and then allowed to cool to room temp. The product was isolated by centrifugation and washed with EtOH. Similarly,
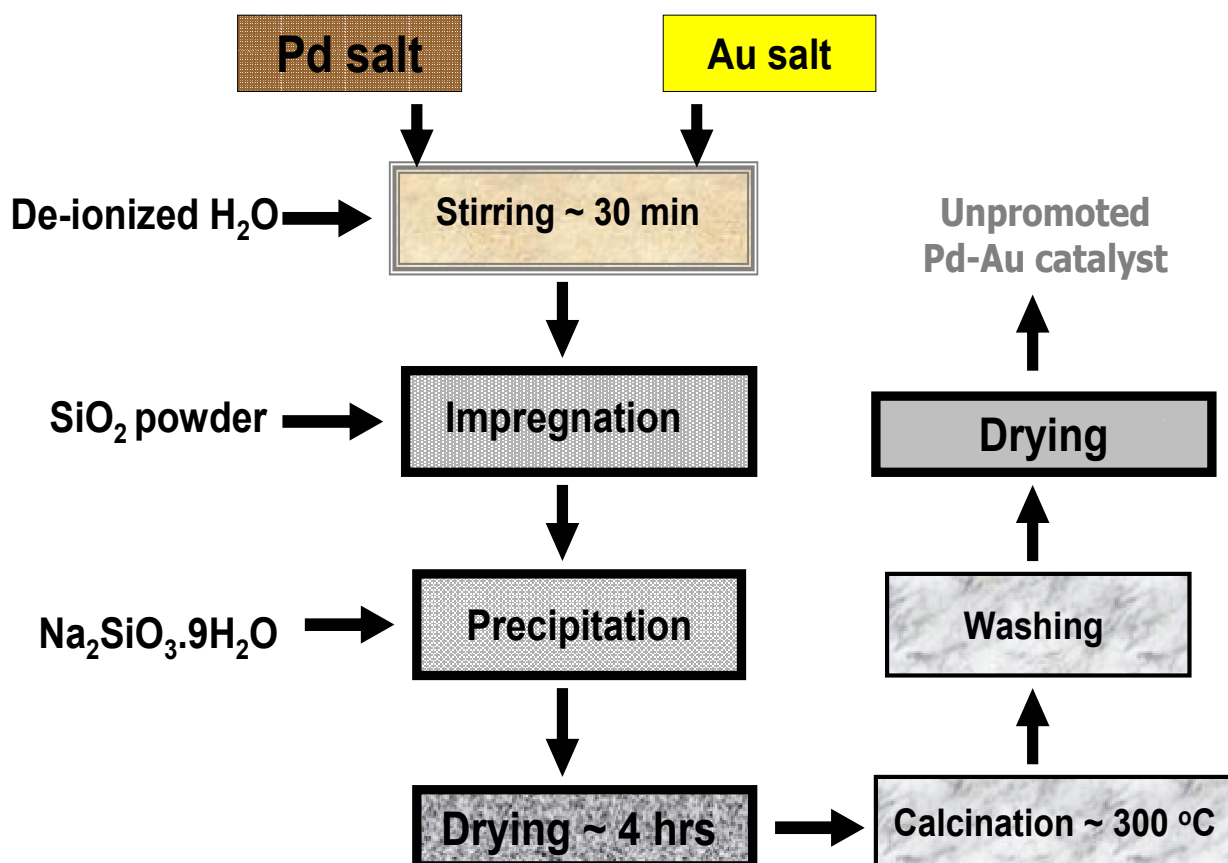
Fig. 9.   Schematic of the synthesis of Pd-Au catalysts using wet impregnation method.

polymer-based catalyst was synthesized using polyvinylpyrrolidone (PVP) polymer instead of sodium acetate in the preparation procedure. N_2, C_2H_4, $O_2(10\%)/N_2$, and air (Messer MG Industries) were purified with gas filters (Chrompack) to remove trace amounts of water, oxygen, and hydrocarbon. Partial pressures of AcOH were maintained by bubbling N_2 through a AcOH (Aldrich C.P.) bath at a preset and regulated temperature.

Experimental Setup

One of the most common ways to carry out a heterogeneous catalyzed gas phase reaction is by passing reactants over a fixed solid phase catalyst. The arrangement of the fixed catalyst is generally called a fixed-bed and the respective reactor is called a fixed-bed reactor [2]. The chemical transformation occurs in a flow reactor through which the gaseous reacting species pass. Atoms on the surface of the catalyst may form chemical bonds (chemisorption) and/or physical bonds (physisorption) with atoms in impinging molecules (reactants). If existing bonds in the impinging molecule break, the process is known as "dissociative chemisorption". The chemisorbed species are mobile on the surface and may bond to other particles, thus leading to new molecules, which eventually leave the surface (desorb) as the desired reaction products. The reason for the continued catalytic activity is that the metal atoms are also mobile along with adsorbed reactants on the metal surface.

In our study, VA synthesis oxidation was carried out using a micro-fixed bed reactor and the experimental setup is shown in Fig. 10. Similarly, CO oxidation was also carried out using a similar experimental setup. The catalytic reactor is a quartz tube with 0.8 cm inner diameter and a catalyst bed of approximately 1- 2 cm in length. The catalyst
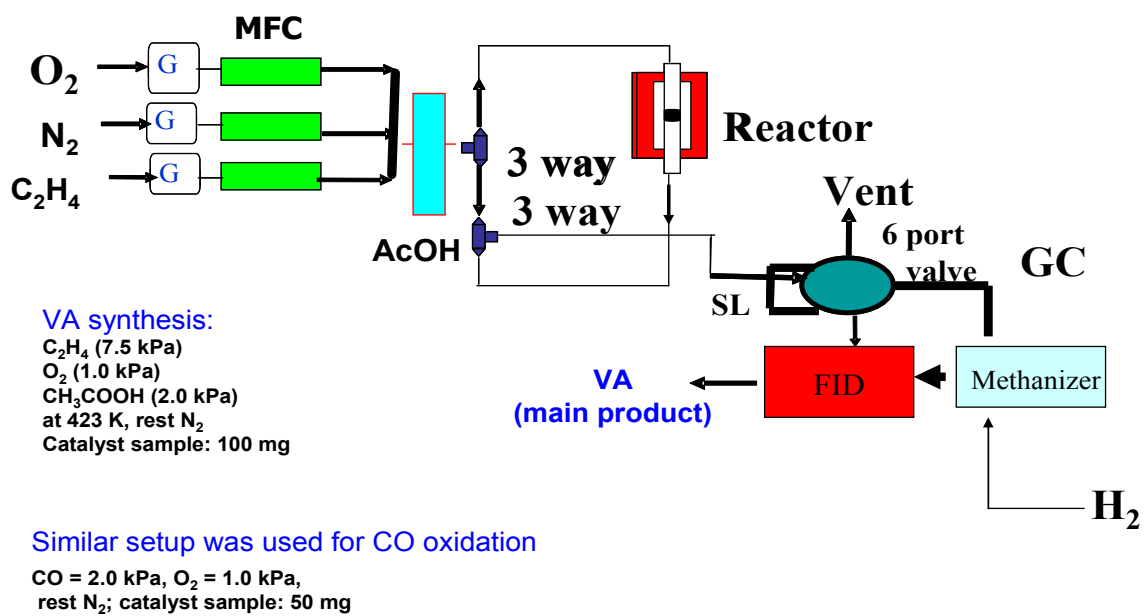
Fig. 10. Experimental setup of micro fixed-bed reactor and accessories.

bed was packed with supported Pd-Au catalyst for VA synthesis and CO oxidation reactions. Mass flow controllers were used to control the gas flow rate. The reactor temperature was regulated using an micromega temperature controller (CN77000 series) and products were analyzed by a HP 5890 GC online gas chromatograph connected to a computing integrator (HP 3393 A). Helium was used as a chemically inert carrier gas. Associated with the gas supply are pressure regulators, gauges, and mass flow meters.

Gas Chromatography (GC)

Chromatographic separation involves the use of stationary phase and a mobile phase. Components of a mixture carried by the mobile phase in the column are differentially attracted by the stationary phase, and thus, move through the stationary phase at different rates and are analyzed by the detectors. The block diagram for the GC unit is shown in Fig. 11. HaySep-R (100/120 mesh) and Porapak-R (80/100 mesh) columns were used to achieve the necessary chromatographic separation. The HaySep-R column with a flame ionization detector (FID) and was used to detect VA and acetic acid. A Porapak-R column connected to a thermal conductance detector (TCD) was used to detect CO and CO_2. In addition, a methanizer was used to detect very small concentrations of CO and CO_2 in the VA synthesis reaction.
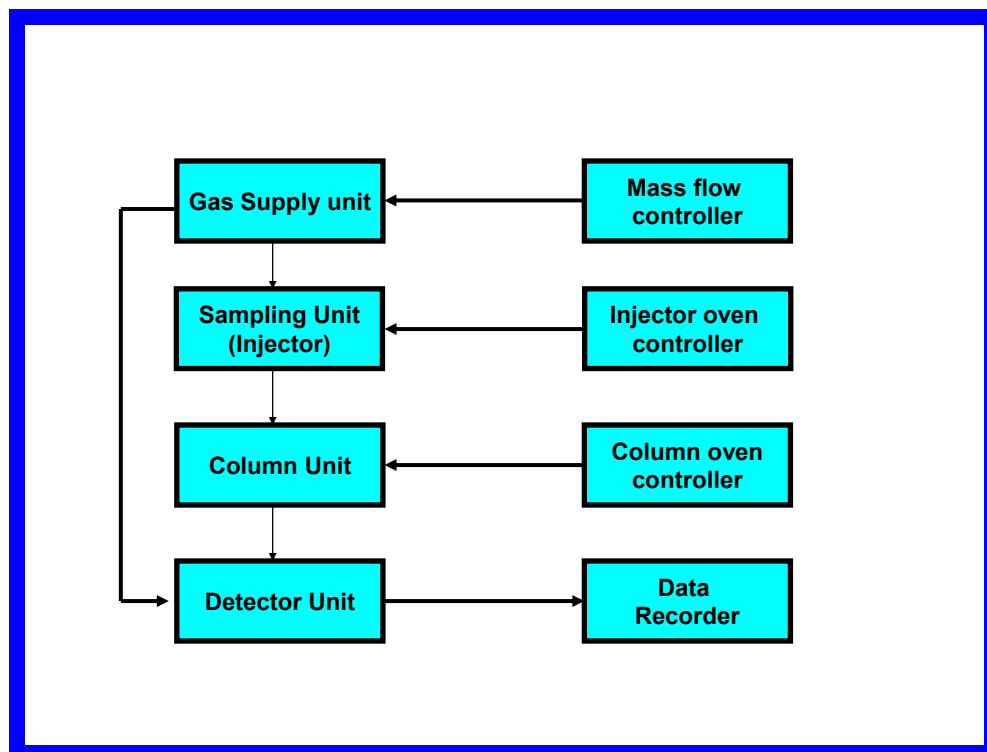
Fig. 11.   Block diagram of gas chromatograph (GC) units

Thermal Conductance Detector (TCD)

TCD is commonly used for fixed gas analyses that include O_2, N_2, CO, CO_2, H_2S and NO. The detector consists of four electrically heated tungsten-rhenium filaments in a Wheatstone bridge configuration as shown in Fig. 12 [39]. The carrier gas flows across the filaments, removing heat at a constant rate. Two of the filaments are exposed only to carrier gas (reference), and two are exposed to the carrier/sample flow. When a sample molecule with lower thermal conductivity than the carrier gas exits the column and flows across the two sample filaments, the temperature of the filaments increases. This temperature increase unbalances the Wheatstone bridge and generates a peak as sample molecules transit through the detector [39]. In our experiment, helium was used as the carrier gas as it has very high thermal conductivity. The flow rate was maintained at 30 ml/min. A TCD was used to detect CO and CO_2 for CO oxidation experiments.

Flame Ionization Detector (FID)

The schematic for the operation of FID is shown in Fig. 13 [40]. A FID detector employs a mixture of hydrogen and air as the combustion gas and burnt as a small jet situated inside a cylindrical electrode [40]. A potential of a few hundred volts, is applied between the sample jet and the electrode. Upon combustion of a carbon containing sample mixture in the jet, electron/ion pairs that are formed are collected at the jet and cylindrical electrode. During the process of oxidation, oxidized or partially oxidized fragments of the sample mixture are formed in the flame and the electrons are generated by thermionic
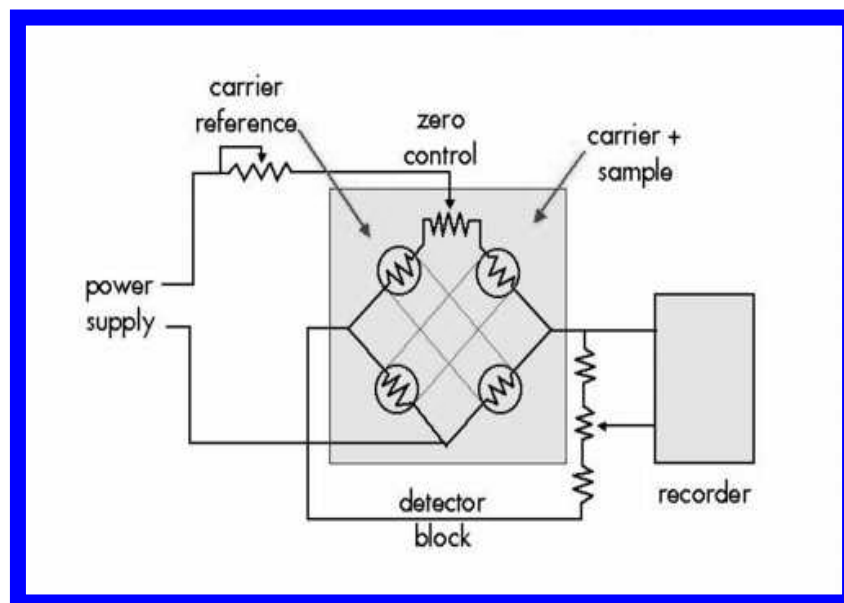
Fig. 12.   Wheatstone bridge configuration of thermal conductivity detector
(Ref. [39]).
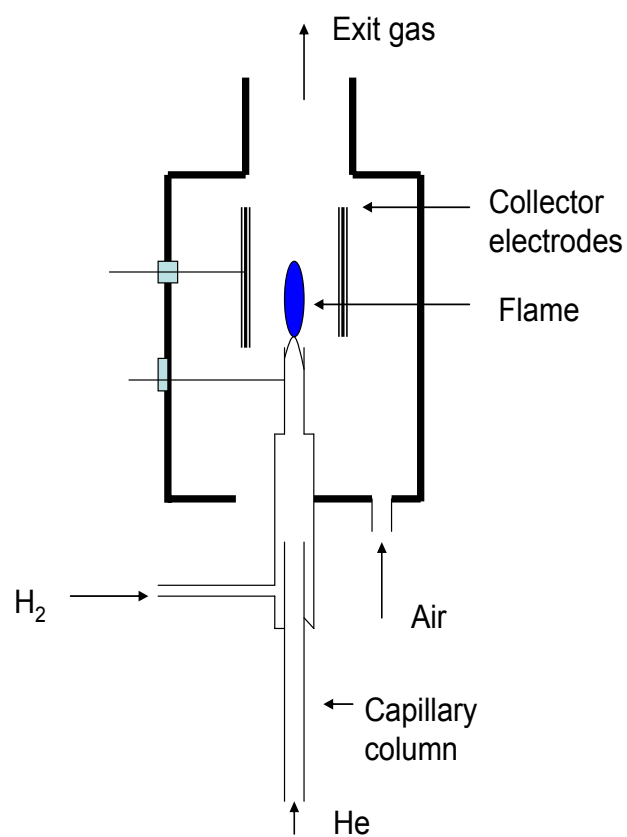
Fig. 13.   The schematic for the operation of flame ionization detector (Ref. [40]).

emission. The background current generated by the ions/electrons from the hydrogen flame is very small compared to the current from a known carbon containing sample mixture. The current is amplified and fed to the computing recorder. In our experiments, the flow rate of hydrogen was maintained at 20 ml/min. The flow rate of helium was maintained at 30 ml/min.

Methanizer

The schematic for the operation of methanizer is shown in Fig. 14. The methanizer accessory enables any GC equipped with a FID to detect low levels of CO and CO_2. The methanizer requires hydrogen for operation and employs a nickel catalyst powder. And during analysis, the methanizer is heated to 380 ^{o}C. Helium (carrier gas) mixed with hydrogen passes through the methanizer to convert CO and CO_2 to methane. The retention times of CO and CO_2 remain unchanged as the conversion of CO and CO_2 to methane occurs after the sample has passed through the column. On the other hand, hydrocarbons pass through the column unaffected. In our experiments, the flow rate of hydrogen was maintained at 20 ml/min.
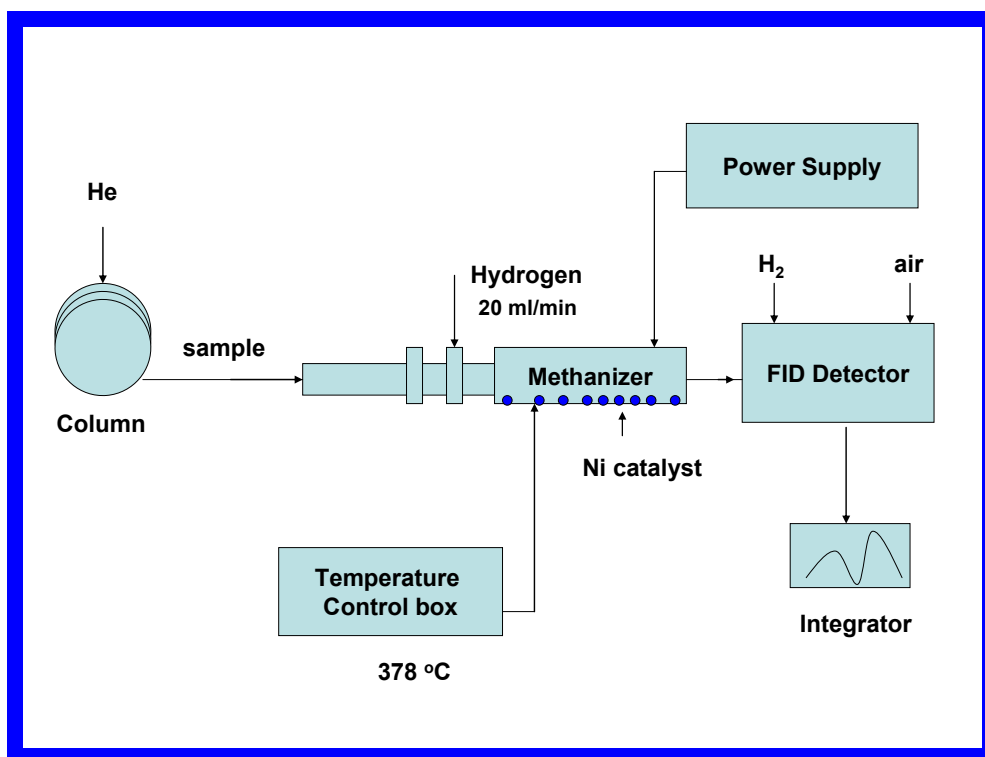
Fig. 14.   The schematic of stand-alone methanizer accessory with FID.

Characterization Techniques

X-Ray Diffraction (XRD)

XRD is a standard tool for the identification and characterization of heterogeneous catalysts. The working principle of X-ray diffraction is shown in Fig. 15 [2]. To understand the principle, let us consider an X-ray beam incident on parallel planes P1 and P2, separated by an interplanar spacing d. The two parallel incident rays, A and B are at an angle (θ) with respect to these planes. A reflected beam of maximum intensity will result if the waves are in phase, represented by A' and B'. The difference in pathlength between A to A' and B to B' must be an integral number of wavelengths (λ). We can express this relationship by Bragg's law [8, 10]:

$$2d \sin \theta = n \lambda \tag{18}$$

where d is the spacing defined by the indices and determined by the geometry of the unit cell. Applying Bragg's law, the particle size of the palladium was calculated from the line broadening of the most intense reflections using the Scherrer formula [8, 10],

$$D = k\lambda / \Delta \cos \theta \tag{19}$$

where λ is the wavelength of the X-rays, k is Scherrer constant, θ is the Bragg angle of the peak maximum, and Δ is the full width at half-maximum (FWHM). In our study, the catalyst was characterized using a Brucker D8 diffractometer employing Cu-K$_\alpha$ radiation. The scanning angle range was 30 to 50° in 0.4 steps.
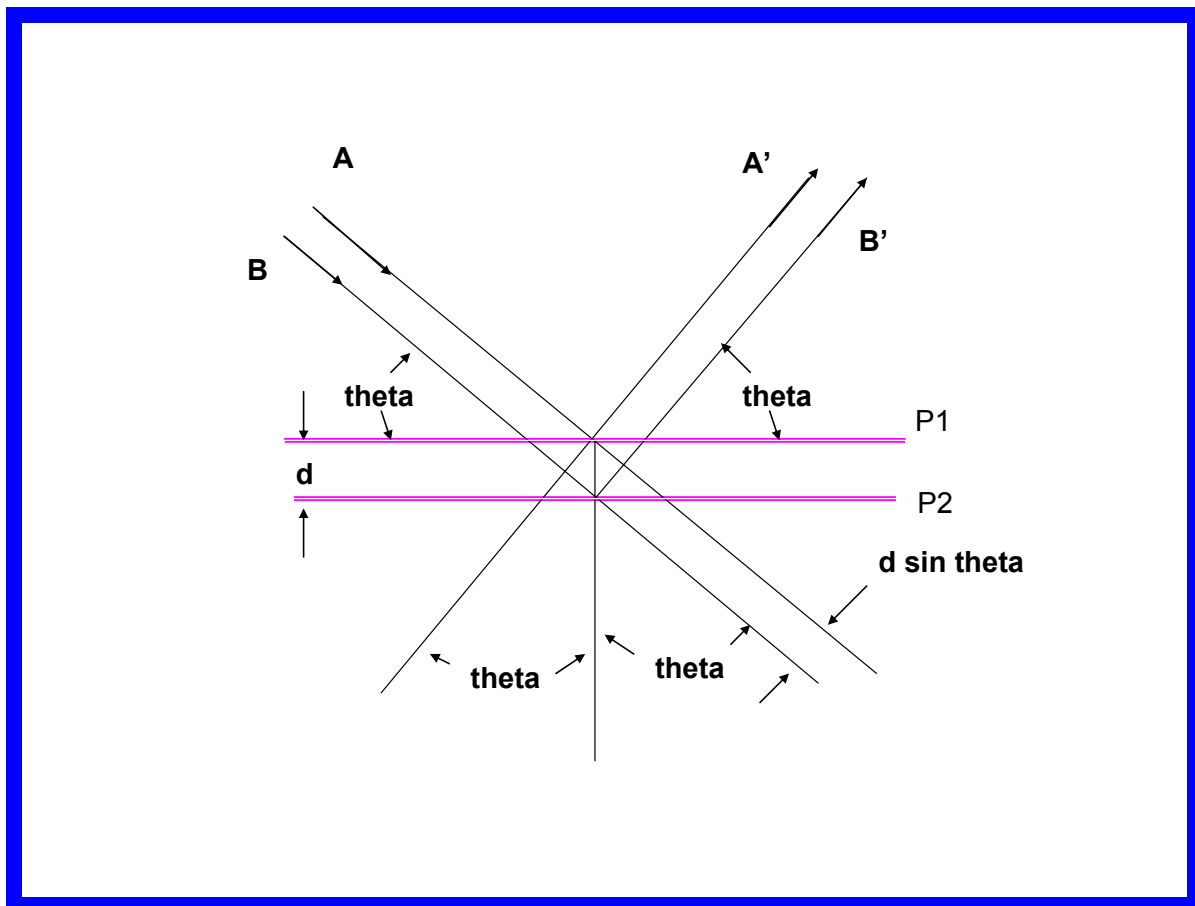
Fig. 15.   Principle of X-ray diffraction (adapted from Ref. [2]).

Transmission Electron Microscopy (TEM)

In TEM, a thin specimen is irradiated with an electron beam of uniform current density as shown in the Fig. 16 [2]. Electrons are emitted from the electron gun and illuminate the specimen through a two or three stage condenser lens system. The objective lens forms a diffraction pattern of the specimen. The electron intensity distribution behind the specimen is magnified with a three or four stage lens system and viewed on a fluorescent screen. The image can be recorded by direct exposure of an image plate by a CCD camera. Since the wavelength of electrons is much smaller than that of light, the optimal resolution attainable for TEM images is many orders of magnitude higher than that from a light microscope. Thus, TEM images can reveal the finest details of internal structure - in some cases as small as individual atoms [11]. In our study, Pd-Au catalyst was ultrasonically dispersed in an ethanol solvent and then dried over a carbon grid. The catalyst was imaged using a Jeol 2010 microscope. 250-300 particles were measured to obtain the average particle-size distribution.
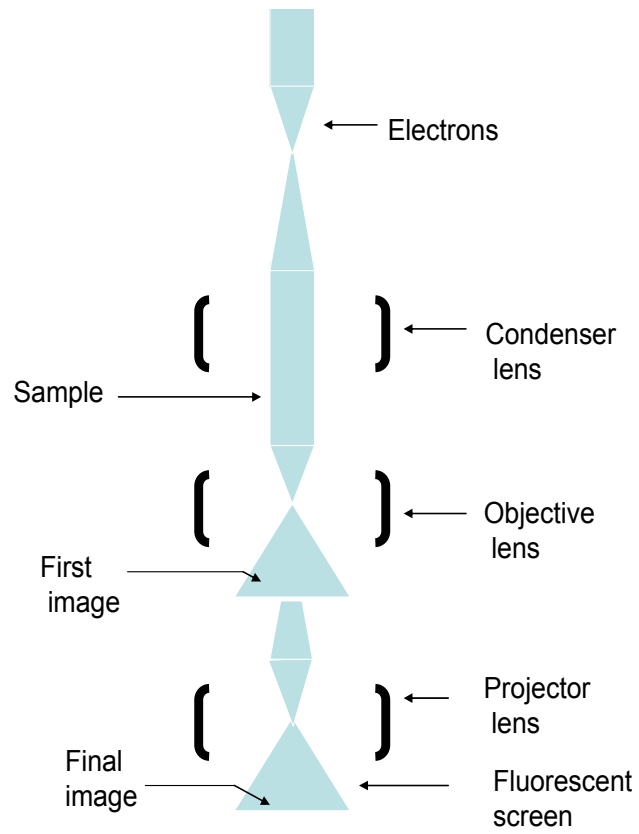
Fig. 16.   Working principle of transmission electron microscopy
            (adapted from Ref. [2]). .

Calculations of the Reaction Rates and Selectivities

C_2H_4 conversion, $X_{C_2H_4} = (p_{C_2H_4} - p_{C_2H_4,in}/p_{C_2H_4,out})$, was calculated from the

CO_2 concentration at the reactor exit:

$$X_{C_2H_4 \to CO_2} = \frac{0.5\, p_{CO_2,out}}{p_{C_2H_4,\ in}} \qquad (20)$$

Under differential flow conditions the mass-normalized reaction rates $r_{C_2H_4}$ can be

calculated directly from the average C_2H_4 partial pressure $\overline{p}_{C_2H_4}$, at the entrance and exit

of the reactor, normalized to the atmospheric pressure p_0, the metal mass in the catalyst

bed, m_{Me}, and the total molar flow rate V_{tot},

$$r_{C_2H_4} = \frac{\overline{p}_{C_2H_4}\, X_{C_2H_4}\, V_{tot}}{p_0 m_{Me}} \quad (mol\ s^{-1}\ g_{Me}^{-1}) \qquad (21)$$

Consequently,

$$r_{C_2H_4 \to CO_2} = \frac{\overline{p}_{C_2H_4'}\, X_{C_2H_4 \to CO_2}\, V_{tot}}{p_0 m_{Me}} \quad (mol\ s^{-1}\ g_{Me}^{-1}) \qquad (22)$$

The VA formation rate is expressed as

$$r_{C_2H_4 \to VA} = \frac{\overline{p}_{C_2H_4'}\, X_{C_2H_4 \to VA}\, V_{tot}}{p_0 m_{Me}} \qquad (23)$$

while

$$X_{C_2H_4 \to VA} = \frac{p_{VA,out}}{p_{C_2H_4,in}} \qquad (24)$$

It should be noted that $r_{C_2H_4 \to CO_2}$ only reflects the conversion rate of C_2H_4 to CO_2. The rate at which ethylene converts to CO_2 is equal to half the CO_2 formation rate. In the present study all CO_2 formation rates are expressed as r_{CO_2}.

In the absence of AcOH, $r_{C_2H_4}$ should be equal to $r_{C_2H_4 \to CO_2}$ and $0.5\,r_{CO2}$, consistent with only ethylene combustion occurring; in the synthesis of VA.

Furthermore, the selectivity S to CO_2 formation is expressed as the fraction of C_2H_4 consumed for CO_2 formation vs the total amount of C_2H_4 consumed, is shown

$$S = \frac{0.5\,p_{CO_2,out}}{p_{C_2H_4,in} - p_{C_2H_4,out}} = \frac{r_{C_2H_4 \to CO_2}}{r_{C_2H_4}} \tag{25}$$

Finally, all the mass-based reaction rates were converted into turn over frequencies, s^{-1} (TOF), according to

$$r_{TOF} = \frac{r_{massbased} M_{Me}}{D} \quad (s^{-1}) \tag{26}$$

M_{me} and D represent the metal atom weight and dispersion of active metal, respectively.

RESULTS AND DISCUSSION

Unpromoted Pd-Au/SiO$_2$ Catalyst

Prior to use, Pd-Au/SiO$_2$ catalyst was pretreated and VA synthesis was carried out using C$_2$H$_4$ (7.5 kPa) and O$_2$ (1.0 kPa) bubbled through CH$_3$COOH (2.0 kPa) at 413 K with the remainder being nitrogen. The weight of the catalyst was 100 mg and the reaction time was approximately 400-600 min.

XRD patterns were obtained for the freshly reduced catalysts as shown in Fig. 17. XRD reveals two diffraction features at Bragg angles of 40.2 and 46.2°, corresponding to polycrystalline Pd(111) and Pd(200), respectively. Using Eq. 19, the particle size for the catalysts was determined to be 4.0 nm. A TEM image was obtained for this catalyst and is shown in Fig. 18. Approximately 250 particles were measured to obtain the average particle-size of 4-5 nm as shown in Fig. 19, which is comparable to XRD results. The corresponding dispersion (29%) was calculated and was used to find the rate of VA formation expressed as a turn over frequency (TOF) or as the number of VA molecules produced per surface active site per second.

VA Synthesis

VA Formation Rate and Selectivity Measurement

VA synthesis was carried out using Pd-Au/SiO$_2$ catalysts and the corresponding rates and selectivities were determined. From Fig. 20 it is evident that the initial reaction rates of Pd-Au/SiO$_2$ catalyst are higher during the first 15 min of the reaction and then the rate reduced. The reaction rate attenuated approximately 3 times its initial rate as is
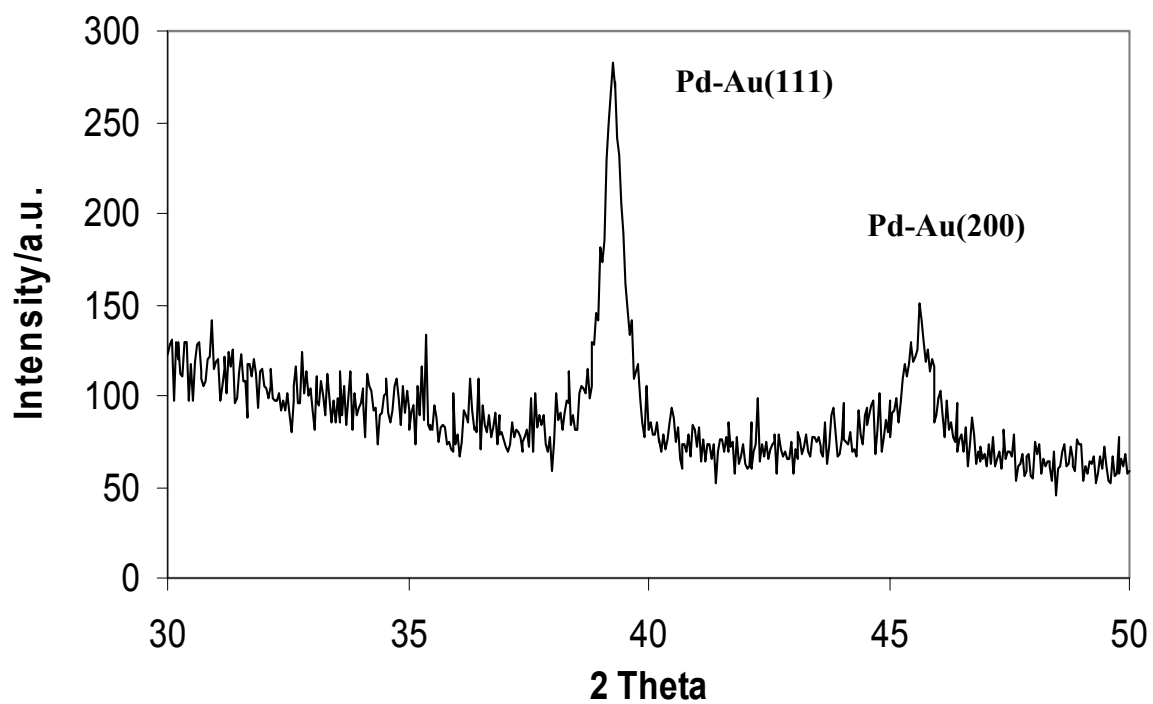
Fig. 17.   XRD data for Pd-Au/SiO$_2$ catalyst after reduction at 673 K in 20 ml/min O$_2$ (10%)/N$_2$, 30 min, then 573 K in 20 ml/min H$_2$ for 30 min.

10 nm
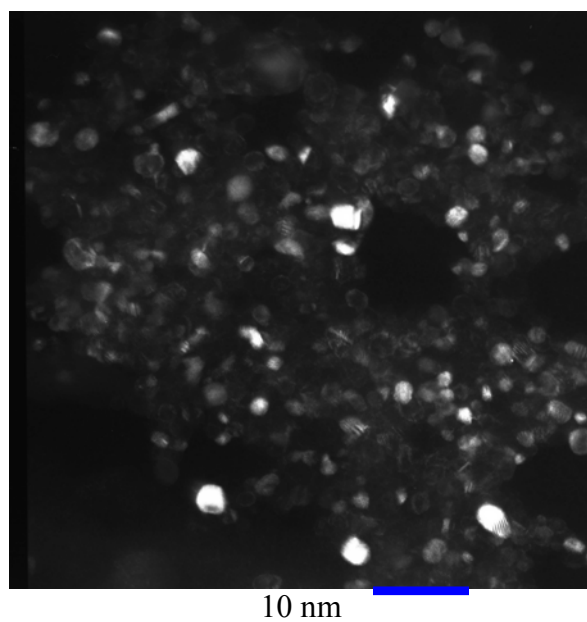
Fig. 18.   TEM micrograph of Pd-Au/SiO$_2$ catalyst after reduction at 673 K in 20
ml/min O$_2$ (10%)/N$_2$, 30 min, then 573 K in 20 ml/min H$_2$ for 30 min.
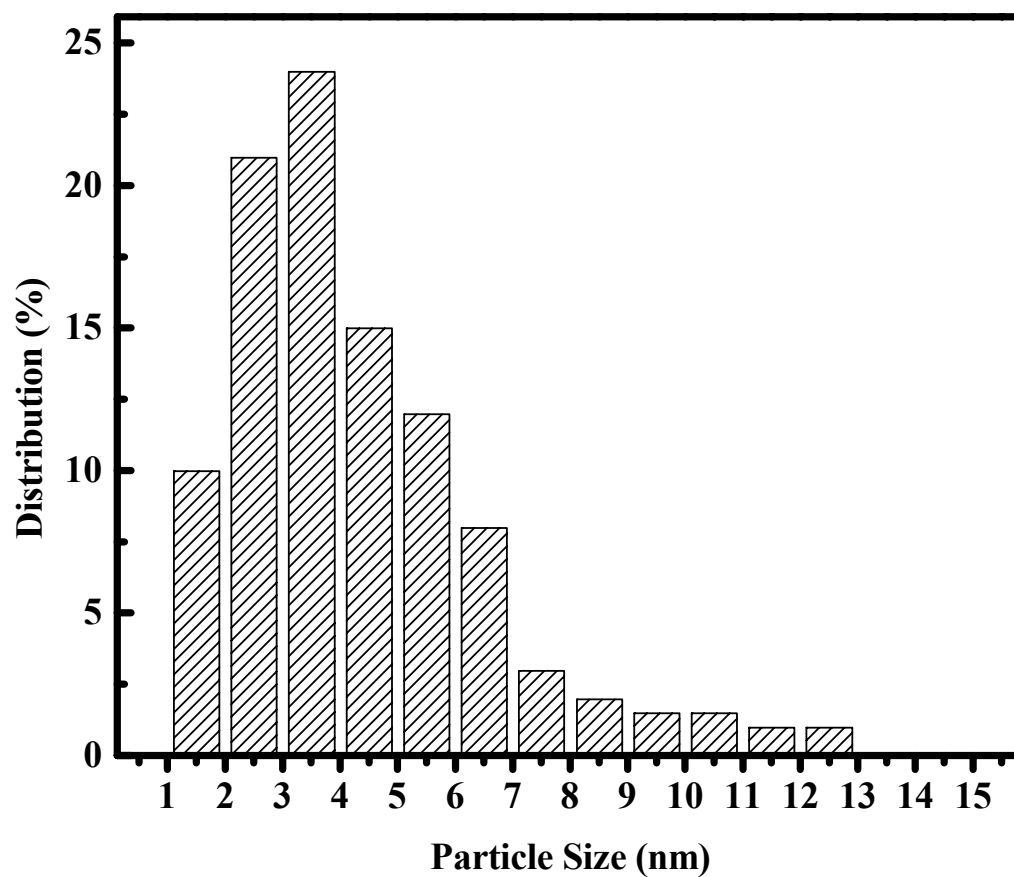
Fig. 19.   Pd-Au cluster distribution of Pd-Au/SiO$_2$ catalyst after reduction at 673 K in 20 ml/min O$_2$ (10%)/N$_2$, 30 min, then 573 K in 20 ml/min H$_2$ for 30 min.
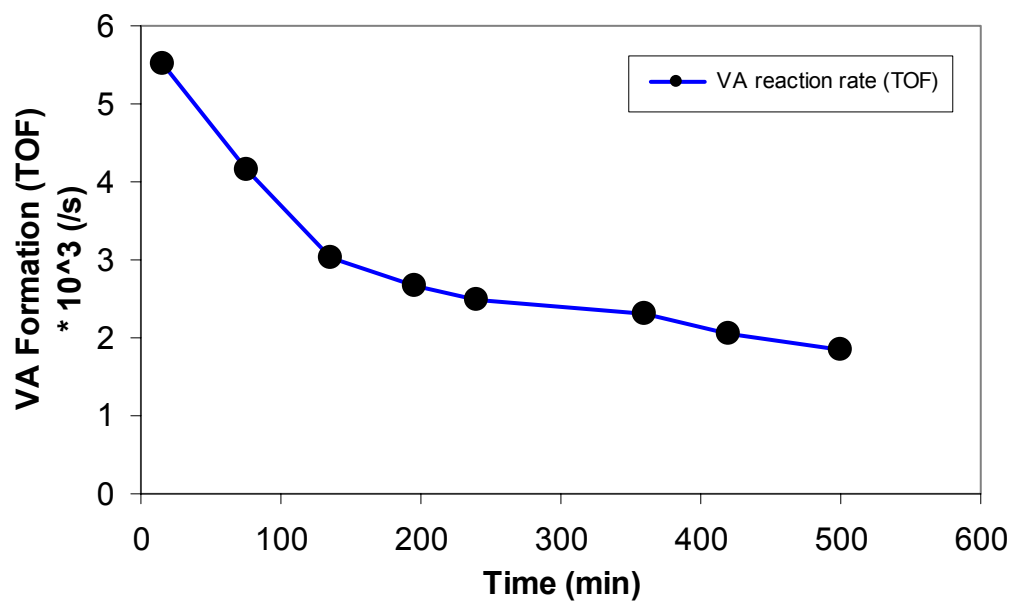
Fig. 20.   Reaction rate of Pd-Au/SiO$_2$ catalyst in the synthesis of vinyl acetate: feed gas, p$_{C_2H_4}$ = 7.5 kPa, p$_{O_2}$ = 1.0 kPa, p$_{AcOH}$ = 2.0 kPa, rest N$_2$; total flow rate, 60 Nml/min at 423 K.
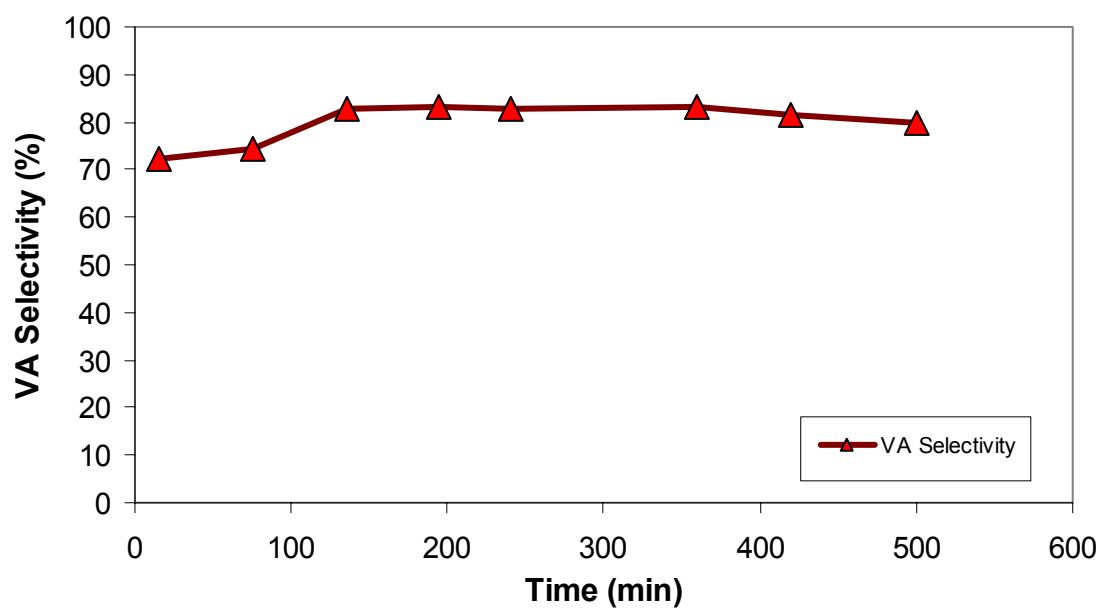
Fig. 21.   Selectivity of Pd-Au/SiO$_2$ catalyst in the synthesis of vinyl acetate: feed gas, p$_{C_2H}$ = 7.5 kPa, p$_{O_2}$ = 1.0 kPa, p$_{AcOH}$ = 2.0 kPa, rest N$_2$; total flow rate, 60 Nml/min at 423 K.

evident between 450-500 min. Therefore Pd-Au/SiO$_2$ catalyst is unstable over a period of 8 hours. On the other hand, the selectivity is approximately 83% as shown in the Fig. 21, in agreement with the previous reports [6]. Therefore, a key improvement in the stability in terms of reaction rate of Pd-Au catalyst is an important step in the current VA synthesis studies.

VA Formation Rate as a Function of Pd-Au Ratio

In our study, various Pd-Au atomic ratios such as Pd (1): Au (1), Pd (1): Au (4), Pd (4): Au (1), Pd (9): Au (1), Pd (1): Au (9), Pd (19): Au (1) and Pd (1): Au (19) were synthesized on a silica support. VA synthesis was carried out using these catalysts and the corresponding reaction rates were measured. From Fig. 22 it is evident that 1: 1 and 4:1 Pd-Au have the higher reaction rates compared to other Pd-Au catalysts. The 4:1 Pd-Au has a higher initial rate than the 1: 1 Pd-Au catalyst but the stability was relatively low. On the other hand, the induction period of the 1: 1 Pd-Au catalyst is higher (~50 min) compared to the 4:1 Pd-Au catalyst. As the Pd concentration is increased the reaction rate is reduced as it is evident from the results for the 9:1 and 19:1 Pd-Au catalysts. Also, as the Au concentration is increased (very low Pd concentration) reduction of the reaction rate is evident from the results for the 1: 4 and 1:19 Pd-Au catalysts. These results match very well the literature results [27] implicating, as the Pd concentration increases, there to be a depletion of isolated Pd sites (more Pd dimers), and a corresponding decrease in the VA reaction rate. On the other hand, if Pd concentration

Fig. 22.   VA formation rates as a function of Pd-Au ratios in the synthesis of vinyl acetate: feed gas, $p_{C_2H_4}$ = 7.5 kPa, p_{O_2} = 1.0 kPa, p_{AcOH} = 2.0 kPa, rest N_2; total flow rate, 60 Nml/min at 423 K.
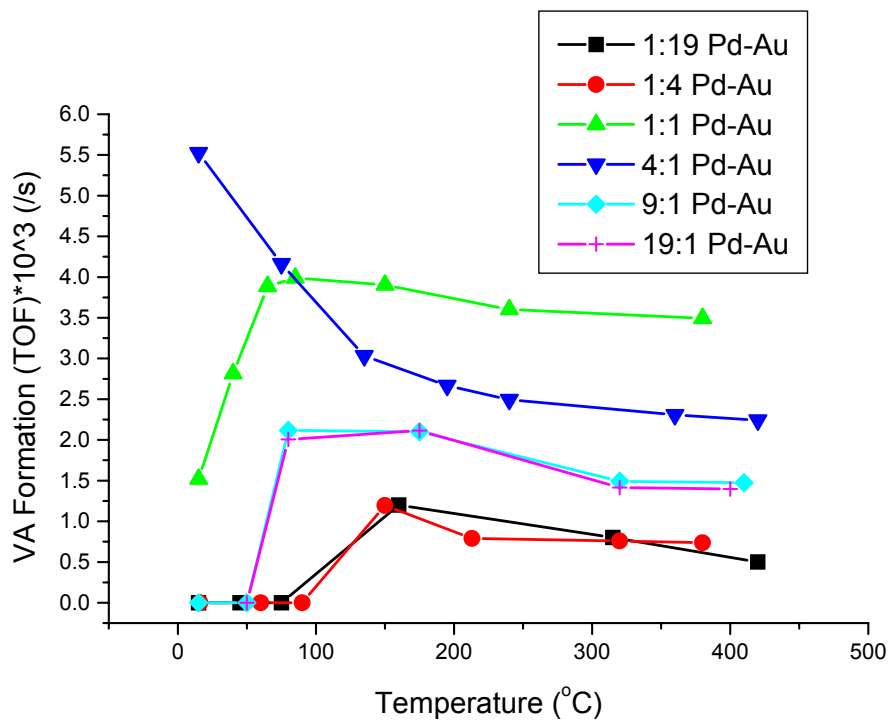
is reduced then Au predominantly covers the surface reducing the VA reaction rate as shown in model systems (Pd<0.07 ML) [27]. Therefore, 1: 1 Pd-Au has the optimum Pd concentration on the surface to produce the higher VA rate followed by 4:1 Pd-Au. Furthermore, 1:1 Pd-Au refers to the bulk concentration of the catalyst. With surface composition of Au ranging from 40% to 96%, this is plausible since a 1:1 Pd-Au has approximately 80% of gold on the surface and isolates Pd sites [7]. These results therefore support isolated Pd sites being catalytically active for VA synthesis.

CO Oxidation

CO Conversion as a Function of Pd-Au Ratio

In this study, we have successfully synthesized supported Pd-Au catalysts with different Pd:Au atomic ratio using incipient wetness methods, then used these catalysts for CO oxidation experiments. The metal loading (5 wt %) was increased to obtain sufficient CO oxidation activity with increased particle sizes. From Fig. 23 it is evident that a supported 1:4 Pd-Au catalyst yields 100% CO conversion at a relatively lower temperature (90 $^{\circ}$C) compared to other Pd-Au ratios. As the palladium concentration increases, CO conversion is reduced as is evident from 2:3, 1:1, 4:1 and 9:1 Pd-Au catalysts. Also, as the Au concentration is increased (very low Pd concentration) the reaction rate is reduced as it is evident from 1: 9 Pd-Au catalyst. These results suggest that enhanced catalytic activity can be obtained for an optimum Pd concentration on the
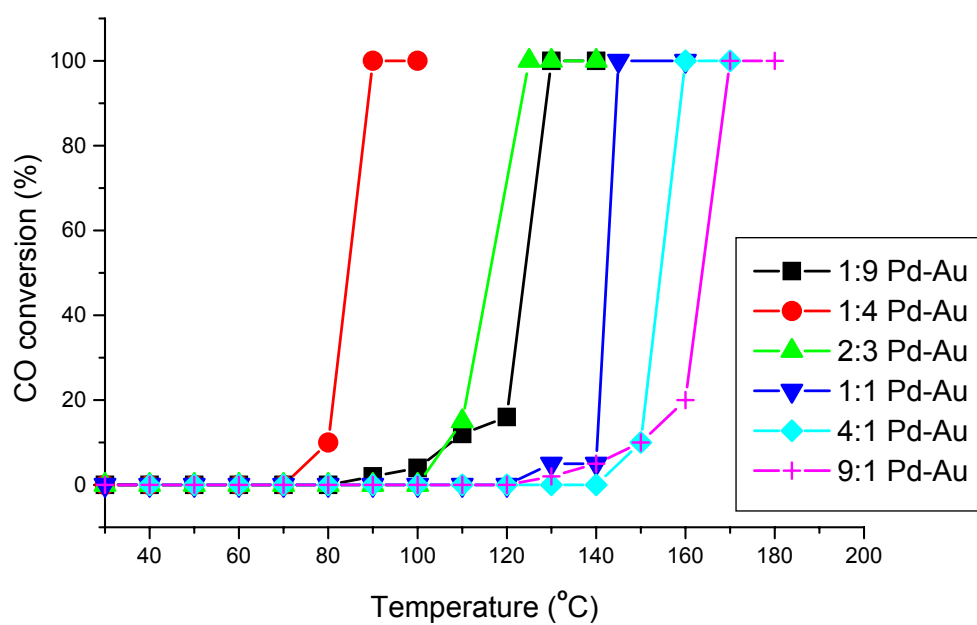
Fig. 23.   CO conversion as a function of temperature for different Pd-Au ratios: feed
gas, $pCO_2 = 2$ kPa, $pO_2 = 1.0$ kPa, rest N_2; catalyst sample: 50 mg.

catalyst surface. Furthermore, these CO oxidation results are similar to the results obtained for VA synthesis by altering the Pd-Au ratio, indicating that isolated Pd sites could be catalytically active for CO oxidation reactions [27].

Promoted Pd-Au/SiO$_2$/K$^+$ Catalyst

The addition of electropositive and/or electronegative elements to a supported metal catalyst promotes significant change in the reactivity and selectivity of the catalyst [4, 41, 42, 43, 44]. The addition of potassium acetate to Pd-Au catalyst on supported catalyst has shown a significant enhancement in the catalytic stability [19]. The promoting influence of potassium acetate was assigned to its ability to aid retention of acetic acid in the liquid layer under reaction conditions [19]. Furthermore, vinyl acetate was not formed with the catalyst impregnated with potassium anions such as potassium chloride. Also, the addition of electronegative impurities, such as, sulfur, to certain metal catalysts has shown a decrease in the reactivity and selectivity of the catalyst [37].

In our current research, the effect of adding potassium acetate to the catalyst to improve the catalyst stability and reactivity was studied. XRD pattern was obtained for freshly reduced catalyst as shown in Fig. 24. XRD reveals two diffraction features at Bragg angles of 40.2 and 46.2°, corresponding to polycrystalline Pd(111) and Pd(200), respectively. Using Eq. 19, the particle size for the catalysts was determined to be 5 nm. TEM data were obtained for this catalyst; one such image is shown in Fig. 25. Approximately 250 particles were measured to obtain the average particle-size of 4.5-5.5 nm, which is comparable to XRD results. We employed a similar particle distribution graph technique to obtain the particle as shown for Pd-Au/SiO$_2$ catalyst.

Fig. 24.   XRD data of Pd-Au/SiO$_2$/K$^+$ catalyst after reduction at 673 K in 20
            ml/min O$_2$ (10%)/N$_2$, 30 min, then 573 K in 20 ml/min H$_2$ for 30 min.

20 nm ▬

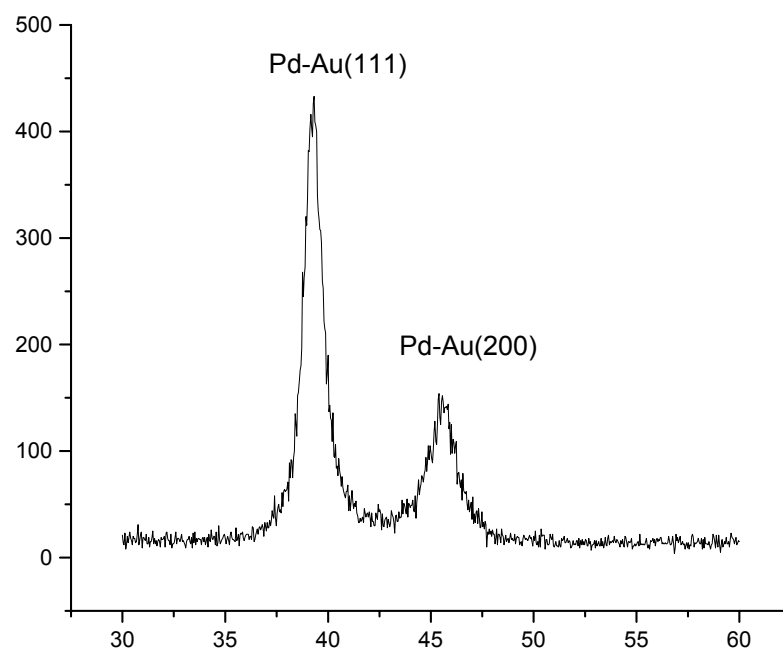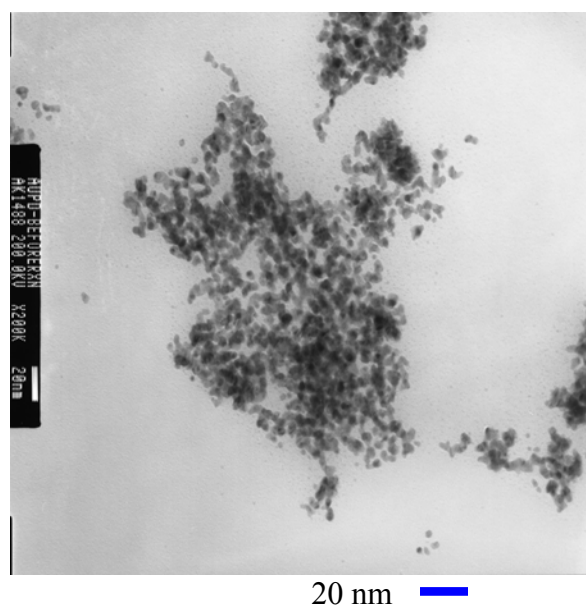Fig. 25.   TEM micrograph of Pd-Au/SiO$_2$/K$^+$ catalyst after reduction at 673 K in 20 ml/min O$_2$ (10%)/N$_2$, 30 min, then 573 K in 20 ml/min H$_2$ for 30 min.

The corresponding dispersion was calculated as 29%, which was used to calculate VA formation rate.

VA Synthesis

VA Formation Rate and Selectivity Measurement

VA reaction rates and selectivities were measured and compared with unpromoted Pd-Au/SiO$_2$ catalyst. From Fig. 26 it is evident that the reaction rate of the promoted Pd-Au/SiO$_2$/K$^+$ catalyst is approximately 40% higher than the unpromoted Pd-Au/SiO$_2$ catalyst. In addition, the promoted catalyst was more stable than the unpromoted catalyst. On the other hand, the unpromoted Pd-Au/SiO$_2$ catalyst was more selective by 5% than the Pd-Au/SiO$_2$/K$^+$ catalyst as shown in Fig. 27. Therefore, addition of promoter (potassium) improves the catalyst stability and reaction rate of the catalyst.

In the current study, we have explored the effect of pre-adsorbed O$_2$, pre-adsorbed acetic acid and the role of O$_2$, which will be important in understanding the rate and selectivity of VA synthesis.
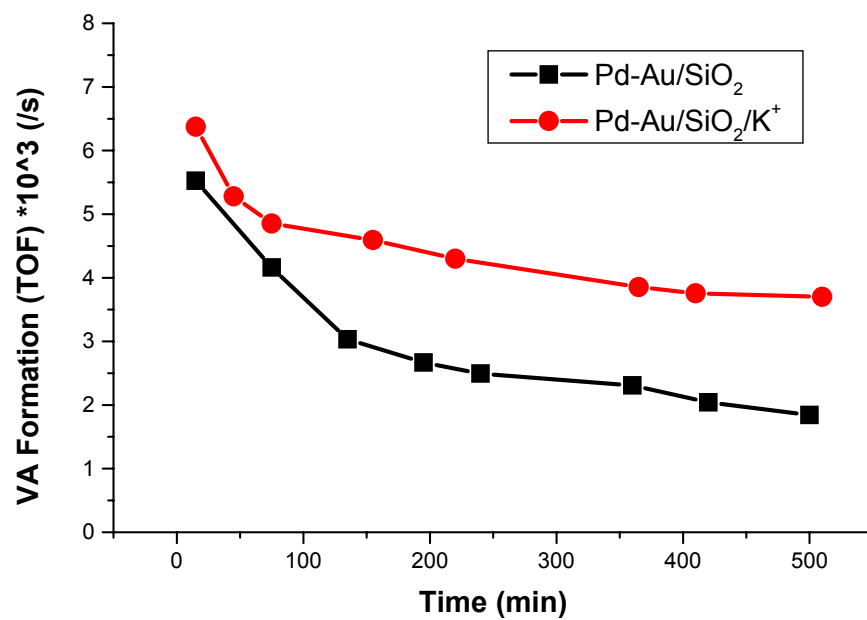
Fig. 26.   Reaction rates ($\bullet$: Pd-Au/SiO$_2$, $\bullet$: Pd-Au/SiO$_2$/K$^+$) in the synthesis of vinyl acetate: feed gas, $p_{C_2H_4}$ = 7.5 kPa, p_{O_2} = 1.0 kPa, p_{AcOH} = 2.0 kPa, rest N$_2$; total flow rate, 60 Nml/min at 423 K.
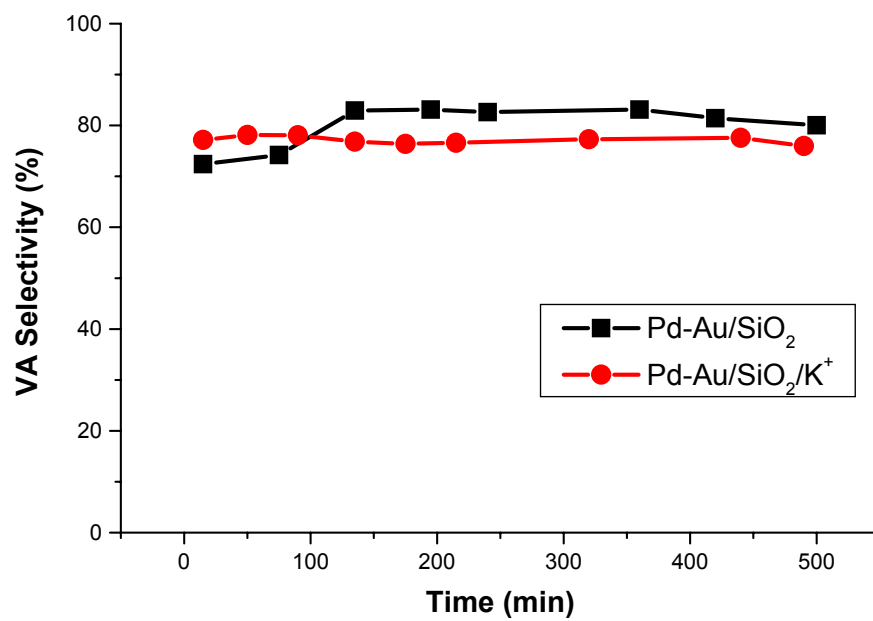
Fig. 27. VA selectivities (■: Pd-Au/SiO$_2$, •: Pd-Au/SiO$_2$/K$^+$) in the synthesis of vinyl acetate: feed gas, p$_{C_2H_4}$ = 7.5 kPa, p$_{O_2}$ = 1.0 kPa, p$_{AcOH}$ = 2.0 kPa, rest N$_2$; total flow rate, 60 Nml/min at 423 K.

Effect of Pre-Treatment

Pre-treatment is an effective way to activate the catalyst and the procedure adopted is oxidizing the catalyst followed by reducing it at a lower temperature. In our current study, the catalyst was pre-treated using 10% O_2/N_2 mixture at 673 K for 30 min with a flow rate of 20 ml/min followed by reduction in 100% H_2 at 573 K. VA synthesis was carried out using pre-treated and un-pretreated Pd-Au/SiO$_2$/K$^+$ catalysts. From Fig. 28 it is evident that the reaction rate of the pre-treated catalyst is approximately 2.5 times higher than the un-pretreated catalyst. Furthermore, the pre-treated catalyst was stable for more than 9 hours. Therefore, in all our studies, the catalyst was pre-treated before use.

Induction Period Measurement

Induction period refers to the initial slow phase of a catalytic reaction which later accelerates. An induction period is observed in these catalytic systems before steady-state concentration of the reactants is reached. Identification of the induction period is a key issue to thoroughly understand the catalytic reaction process. In our experiment, we have successfully measured the induction period of the Pd-Au/SiO$_2$/K$^+$ catalyst. VA synthesis was carried out using a pre-treated Pd-Au/SiO$_2$/K$^+$ catalyst. From Fig. 29 it is evident that the reaction rate is maximum at a time equal to 15 min and then the reaction rate is reduced by 25% as is evident between 100-400 min. Also, the reaction rate was lower initially (before 15 min) as is evident between 7-14 min. Therefore, these results suggest that Pd-Au/SiO$_2$/K$^+$ has a low induction period (~15 min), which makes it very efficient for VA synthesis.
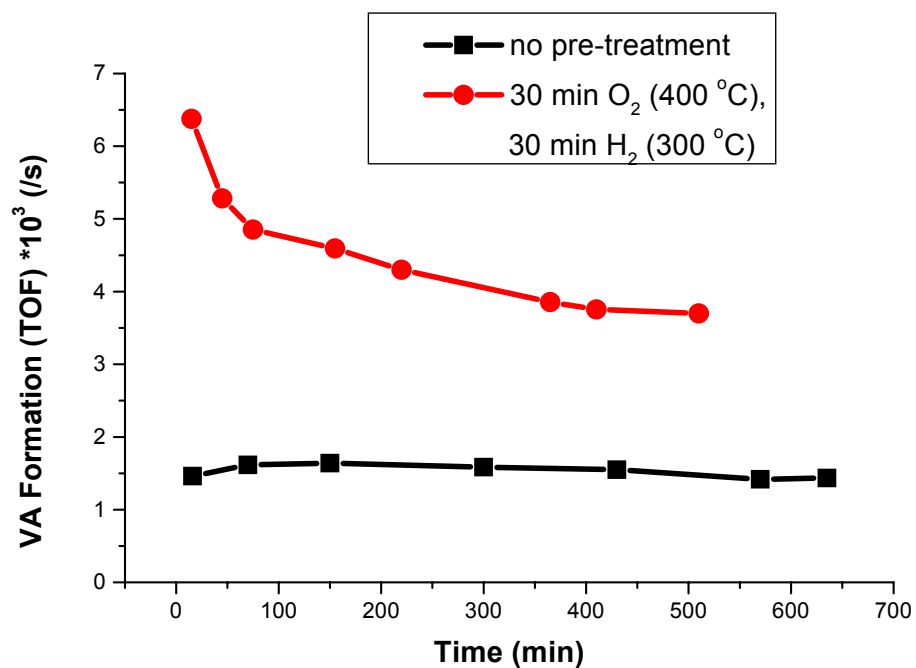
Fig. 28. Reaction rates of Pd-Au/SiO$_2$/K$^+$ catalyst with (▪) and without (•) pre-treatment in the synthesis of vinyl acetate: feed gas, p$_{C_2H_4}$ = 7.5 kPa, p$_{O_2}$ = 1.0 kPa, p$_{AcOH}$ = 2.0 kPa, rest N$_2$; total flow rate, 60 ml/min at 423 K.

Fig. 29.   Induction period measurement of Pd-Au/SiO$_2$/K$^+$ catalyst in the synthesis of vinyl acetate: feed gas, p$_{C_2H_4}$ = 7.5 kPa, p$_{O_2}$ = 1.0 kPa, p$_{AcOH}$ = 2.0 kPa, rest N$_2$; total flow rate, 60 Nml/min at 423 K.

Therefore, in all our VA synthesis studies, the first reaction rate measurement was made within 15 minutes of the reaction time.

Effect of Pre-Adsorbed Oxygen

This study explores the effect of pre-adsorbed oxygen on the VA formation rate of the catalyst. It was observed that the coadsorption of oxygen with acetate essentially eliminated the acetic acid catemers on the Pd [20]. In addition, surface oxygen was found to stabilize acetate binding and inhibit acetate decomposition kinetics. Bond order conservation principles suggest that the most favorable interaction between surface oxygen and acetate would be one in which two adsorbates are one surface Pd-Pd bond removed from one-another. Therefore, this should give rise to enhanced acetate adsorption. On the other hand, similar rate constants were obtained for VA synthesis reactions using monometallic model Pd (111) catalysts surface in the presence and absence of pre-adsorbed oxygen [45, 46].

In our experiment, the reaction rate was explored in the presence and absence of pre-adsorbed oxygen using a $Pd-Au/SiO_2/K^+$ catalyst. Pre-covered oxygen surface was prepared by passing oxygen through the pre-treated catalyst for 30 min under reaction conditions. From Fig. 30 it is evident that the VA rates are similar in the presence and absence of pre-adsorbed oxygen as is evident between 15-400 min. Therefore pre-adsorbed oxygen does not have an effect in VA formation rate, which agrees well with the literature results [45, 46].
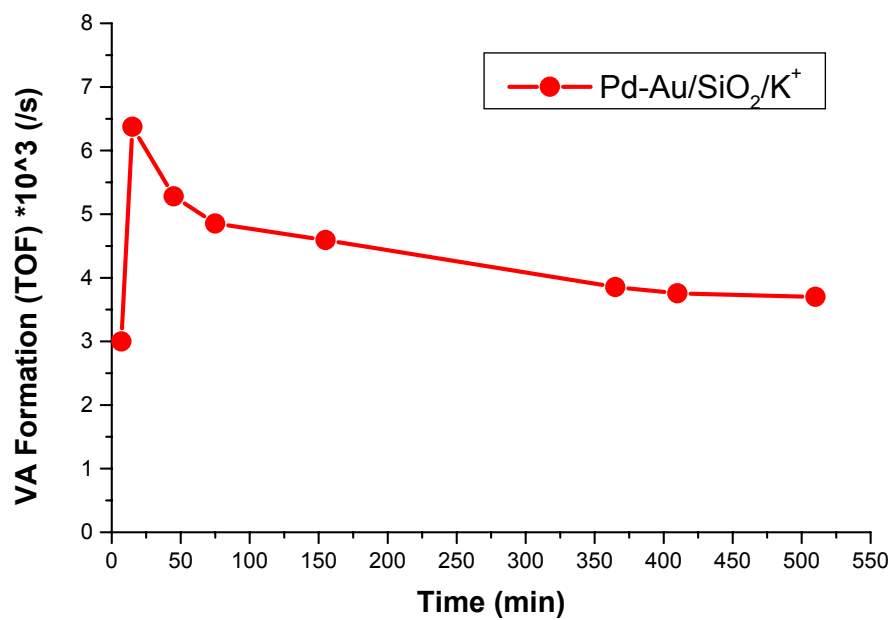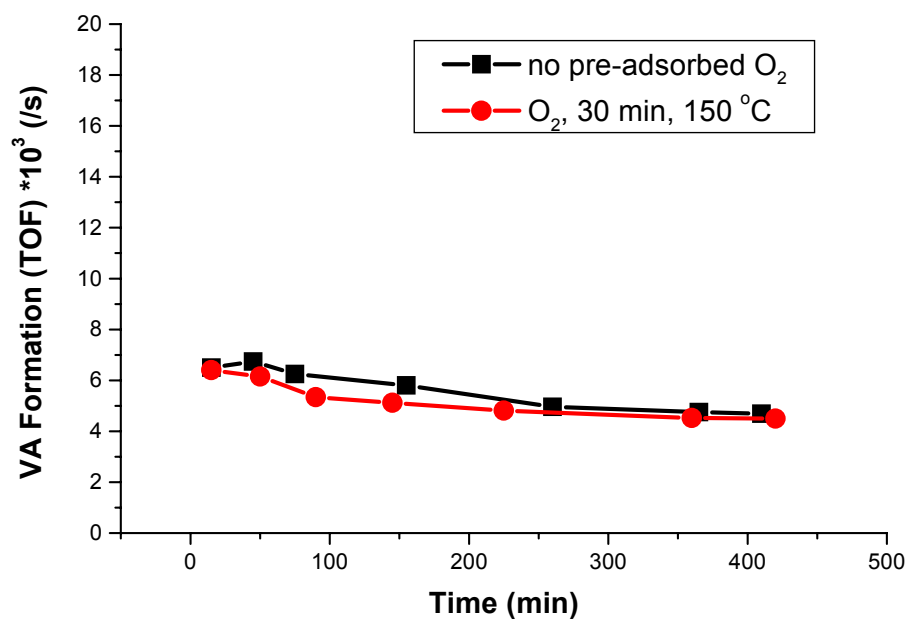
Fig. 30.   Reaction rates of Pd-Au/SiO$_2$/K$^+$ catalyst in the presence (•) and absence (▪) of pre-adsorbed oxygen in the synthesis of vinyl acetate: feed gas, p$_{C_2H_4}$ = 7.5 kPa, p$_{O_2}$ = 1.0 kPa, p$_{AcOH}$ = 2.0 kPa, rest N$_2$; total flow rate, 60 Nml/min at 423 K.

Effect of Pre-Adsorbed Acetic Acid

It is believed that VA catalysts are covered by a liquid-like film of acetic acid and water equivalent to approximately three molecular layers [47, 48]. As mentioned earlier, potassium acetate promotes the retention of acetic acid in the liquid layer [19]. Therefore, VA synthesis was carried out as a function of pre-adsorbed acetic acid. In our experiment, pre-adsorbed acetic acid surface was prepared by bubbling nitrogen through acetic acid over a Pd-Au/SiO$_2$/K$^+$catalyst surface for 30, 60 and 120 min under reaction conditions. The corresponding reaction rates of this catalyst are compared with a freshly reduced Pd-Au/SiO$_2$/K$^+$ catalyst as shown in Fig. 31. The freshly reduced catalyst had higher reaction rate compared with catalyst pre-adsorbed with acetic acid. These results strongly imply that pre-adsorbed acetic acid does not have an effect in increasing the reaction rate. Furthermore, the VA reaction rate decreased as the pre-adsorbed acetic acid time was increased.
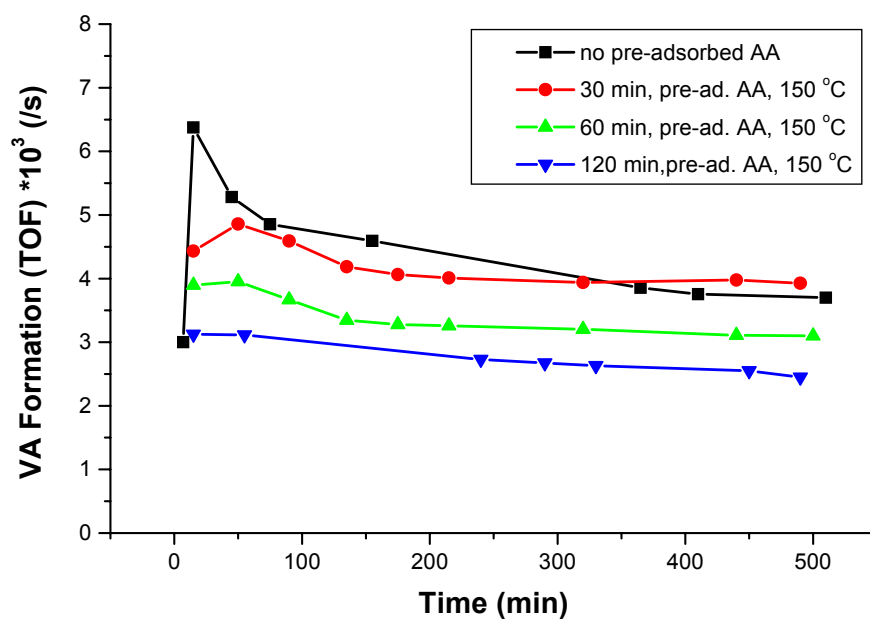
Fig. 31.   VA formation rates as a function of pre-adsorbed acetic acid (AA) in the synthesis of vinyl acetate: feed gas, $p_{C_2H_4} = 7.5$ kPa, $p_{O_2} = 1.0$ kPa, $p_{AcOH} = 2.0$ kPa, rest N_2; total flow rate, 60 Nml/min at 423 K.

Role of Oxygen

It is known that atomic oxygen can induce acetic acid adsorption on metal surfaces [49, 50, 51]. The corresponding stoichiometric equation is given by

$$2CH_3COOH + O\ (a) \rightarrow 2CH_3COO\ (a) + H_2O \tag{27}$$
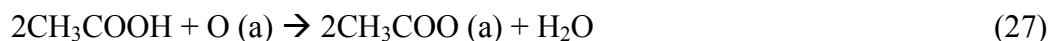
It is evident that pre-adsorbed oxygen does not play any other major role in the VA synthesis reaction except in activating the acetic acid by abstracting an H-atom [4]. It was also shown by XRD studies that no vinyl acetate is formed on a Pd black catalyst in the absence of oxygen [19]. IR results also suggest that oxygen is responsible for the formation of bidentate acetic acid, and thereby, facilitates palladium acetate formation during VA synthesis reaction. Fig. 32 shows the IRAS of acetic acid on oxygen-covered 4 ML Pd/Au alloy surface annealed at 600 K. Without oxygen, a relatively small IR feature of acetic acid is observed. However, in the presence of oxygen, IRAS data show two stretching features at 1710 and 1415 cm^{-1} which are assigned to monodentate and bidentate species adsorbed on Pd surface. Furthermore, TPD results (Fig. 33) show that the monodentate species is desorbed at lower temperature (235 K). On the other hand, the bidentate species desorbs at higher temperature (295 K).

Our results also support the argument that oxygen is an important species in activating acetic acid during VA synthesis. In our experiment, VA synthesis was carried out using a Pd-Au/SiO$_2$/K$^+$ catalyst and oxygen was pulsed during the synthesis. It is evident that VA is produced during the first 200 minutes of the reaction in the presence of oxygen as shown in Fig. 34. The VA rate is reduced to zero when the flow of oxygen was stopped as is evident between 200-300 min.
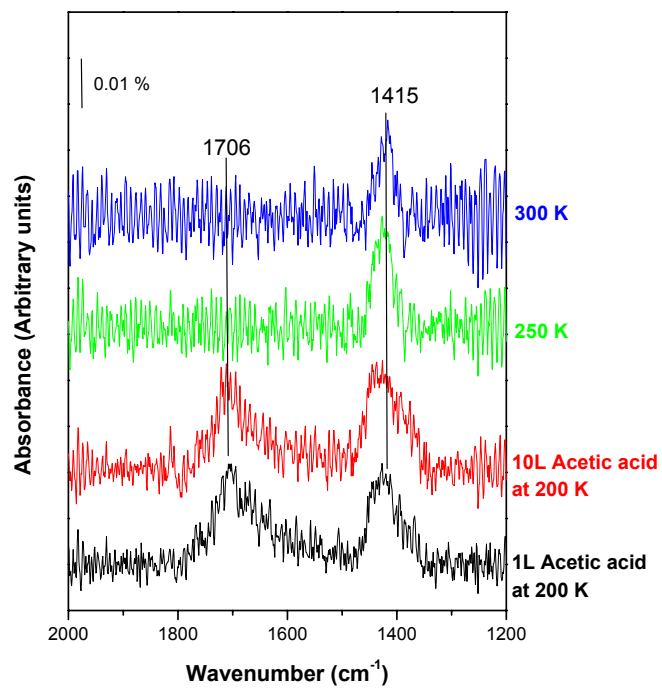
Fig. 32.   IRAS of acetic acid dosed at 200 K on oxygen pre-covered 4 ML Pd/Au(100) annealed at 600 K.
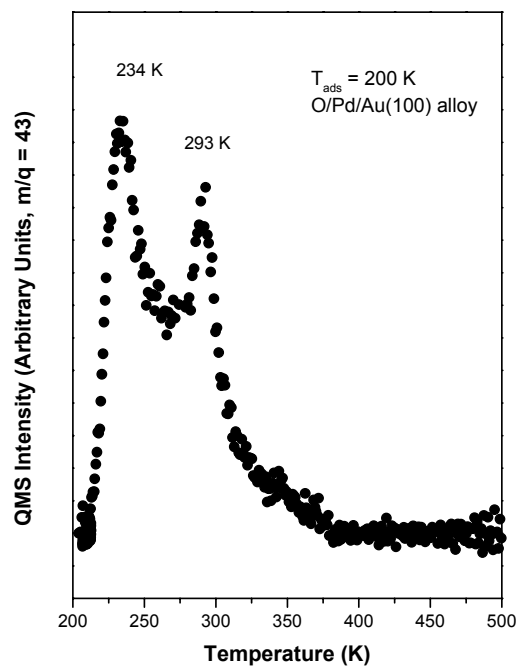
Fig. 33.   TPD of acetic acid dosed at 200 K on oxygen pre-covered 4 ML Pd-Au(100)
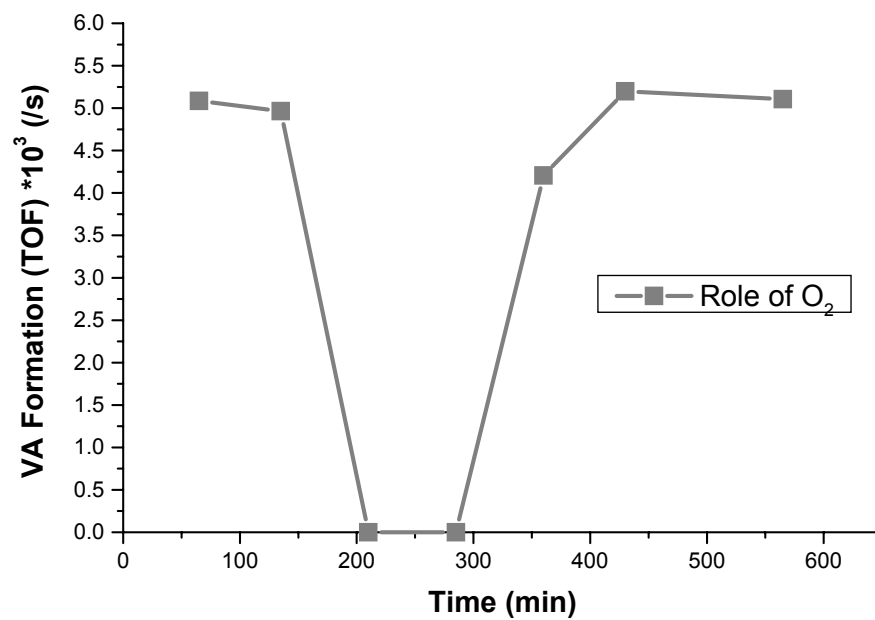   annealed at 600 K.

VA production increased to the initial rate when the oxygen is introduced again confirming that O_2 is an important species in activating acetic acid by H-abstraction [19].

Acetate-Based Pd-Au Catalyst

Although acetoxylation of ethylene to VA on a Pd-Au/SiO_2 catalyst promoted with potassium acetate is a well established industrial reaction, the existing catalysts can be improved with respect to activity and selectivity.

In VA synthesis, KOAc is used as the promoter to increase VA formation rate. As mentioned, the promoting influence of acetate has been correlated with its ability to promote retention of acetic acid in the liquid layer under reaction conditions [47]. Also, acetate enables the formation of palladium acetate dimers which are the active species for VA synthesis [41]. The reaction pathway is given by [41]:

$$2Pd_3(OAc)_6 + 6AcO^- \rightarrow 3[Pd_2(OAc)_6]^{2-} \tag{28}$$

Furthermore, the influence of the acetate anion of various metals have been well studied [19]. Na^+ metal ion combined with acetate ion increase the VA reaction rate on Pd black catalyst [19]. In our current study, VA synthesis was carried out using acetate-based Pd-Au/SiO_2 catalysts, synthesized using a novel centrifuge technique described above. The corresponding reaction rates and selectivity were then measured. XRD patterns were obtained for freshly reduced catalysts as shown in Fig. 35. XRD reveals two diffraction features at Bragg angles of 40.2 and 46.2°, corresponding to polycrystalline Pd(111) and Pd(200), respectively. Using Eq. (19), the particle size for the catalysts was determined to be 18.5 nm.
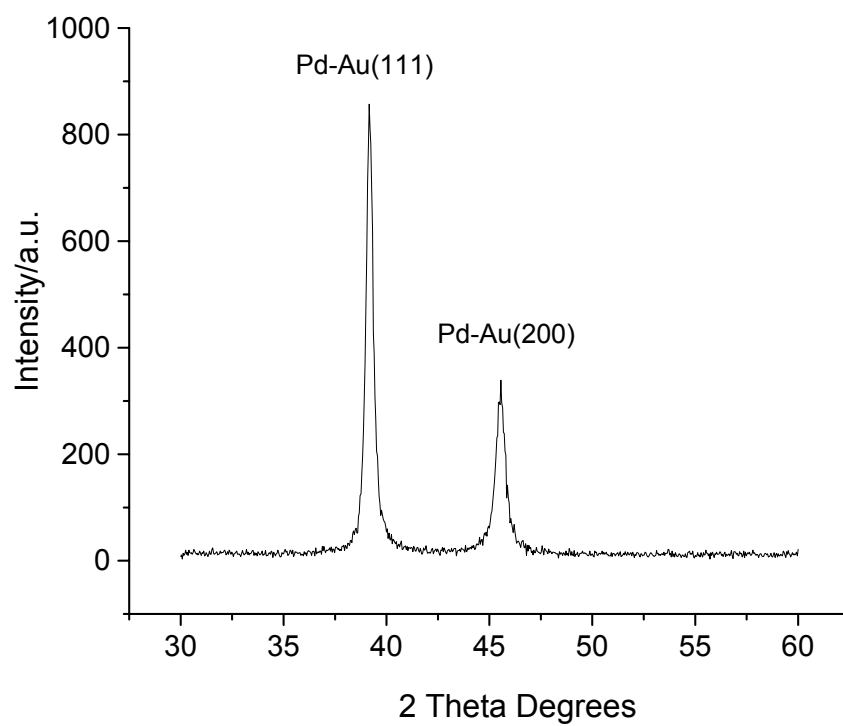
Fig. 35.   XRD data for acetate-based Pd-Au/SiO$_2$ catalyst after reduction at 673 K in 20 ml/min O$_2$ (10%)/N$_2$, 30 min, then 573 K in 20 ml/min H$_2$ for 30 min.
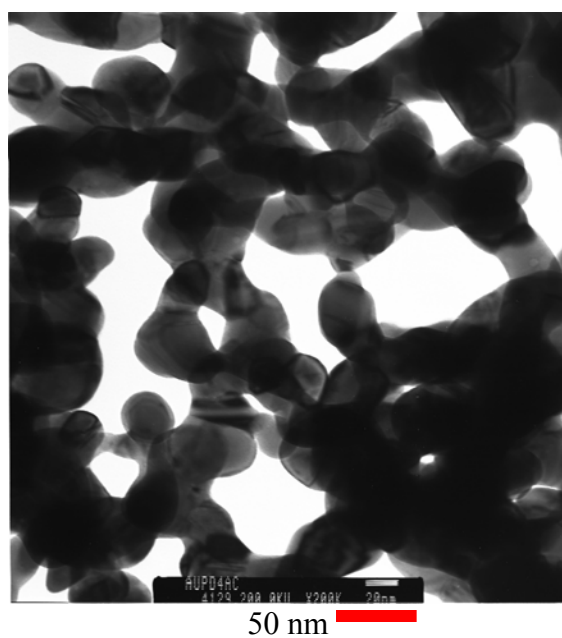
50 nm

Fig. 36.   TEM micrograph of acetate-based Pd-Au/SiO$_2$ catalyst after reduction at 673 K in 20 ml/min O$_2$ (10%)/N$_2$, 30 min, then 573 K in 20 ml/min H$_2$ for 30 min.

Also, TEM images were obtained for this catalyst, one of which is shown in Fig. 36. 250 particles were measured to obtain the average particle-size of 19.5 nm, results comparable to those obtained by XRD.

VA Synthesis

VA Formation Rate and Selectivity Measurement

In our study, we have made significant attempts to improve the Pd-Au based catalyst and compare the activity with the existing promoted and unpromoted Pd-Au/SiO$_2$ catalysts. VA synthesis was carried out using acetate-based Pd-Au/SiO$_2$ and the corresponding VA activity measured, as shown in Fig. 37. The selectivity was also measured, as shown in Fig. 38. Furthermore, the reaction rate and selectivity of acetate-based Pd-Au/SiO$_2$ was compared to that of conventional promoted and unpromoted Pd-Au/SiO$_2$ catalysts. From Fig. 39 it is evident that the reaction rate of acetate-based Pd-Au/SiO$_2$ is approximately 3.5 times higher than Pd-Au/SiO$_2$ and Pd-Au/SiO$_2$/K$^+$ catalysts and is stable for a period of more than 8 hours. Unfortunately the selectivity of the acetate-based Pd-Au/SiO$_2$ catalyst was lower than the Pd-Au/SiO$_2$ and Pd-Au/SiO$_2$/K$^+$ catalysts (Fig. 40).

Fig. 37.   Reaction rates (■: acetate-based Pd-Au/SiO$_2$) in the synthesis of vinyl acetate: feed gas, $p_{C_2H_4}$ = 7.5 kPa, p_{O_2} = 1.0 kPa, p_{AcOH} = 2.0 kPa, rest N$_2$; total   flow rate, 60 ml/min at 423 K.
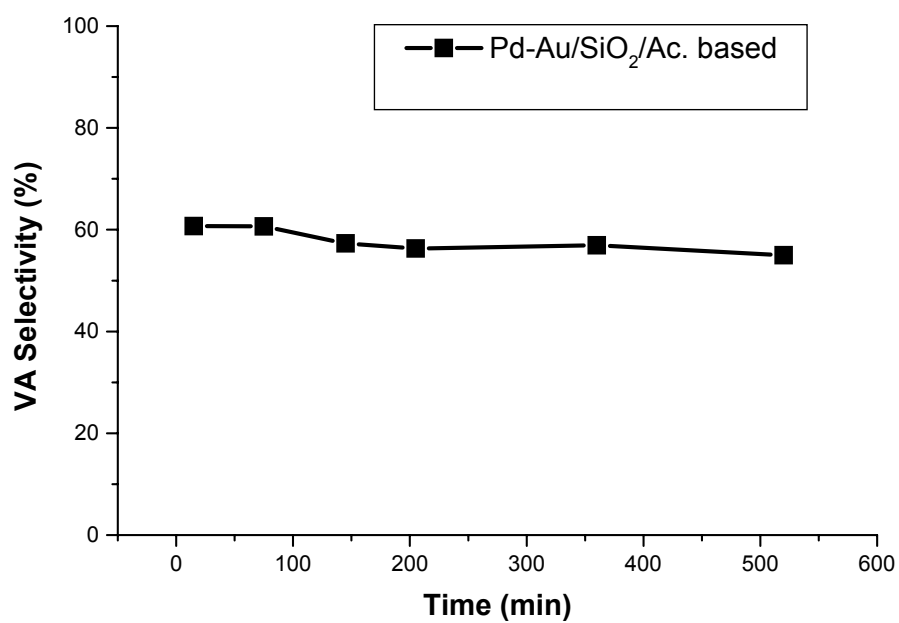
Fig. 38.　VA selectivities (▪: acetate-based Pd-Au/SiO₂)in the synthesis of vinyl acetate: feed gas, $p_{C_2H_4}$ = 7.5 kPa, p_{O_2} = 1.0 kPa, p_{AcOH} = 2.0 kPa, rest N_2; total flow rate, 60 Nml/min at 423 K.
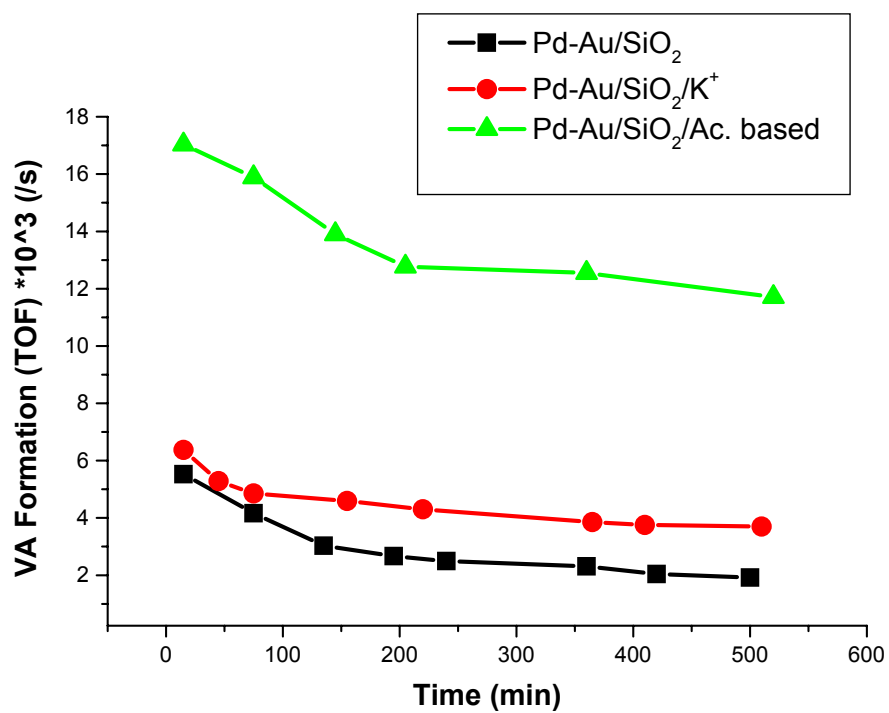
Fig. 39.   Reaction rates (▪: Pd-Au/SiO₂, •: Pd-Au/SiO₂/K⁺, ▲: acetate-based Pd-
Au/SiO₂) in the synthesis of vinyl acetate: feed gas, $p_{C_2H_4}$ = 7.5 kPa, p_{O_2} = 1.0
kPa, p_{AcOH} = 2.0 kPa, rest N_2; total flow rate, 60 ml/min at 423 K.
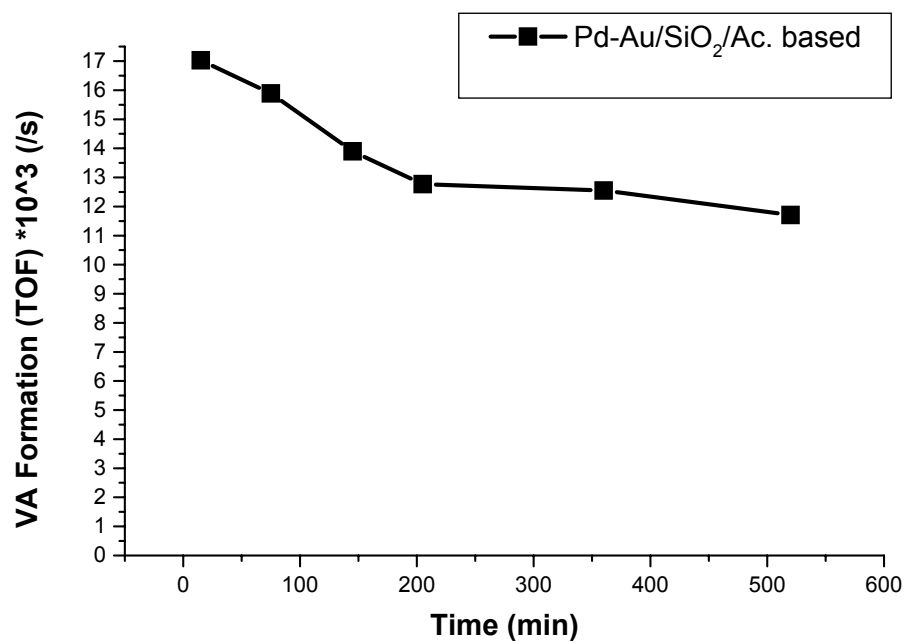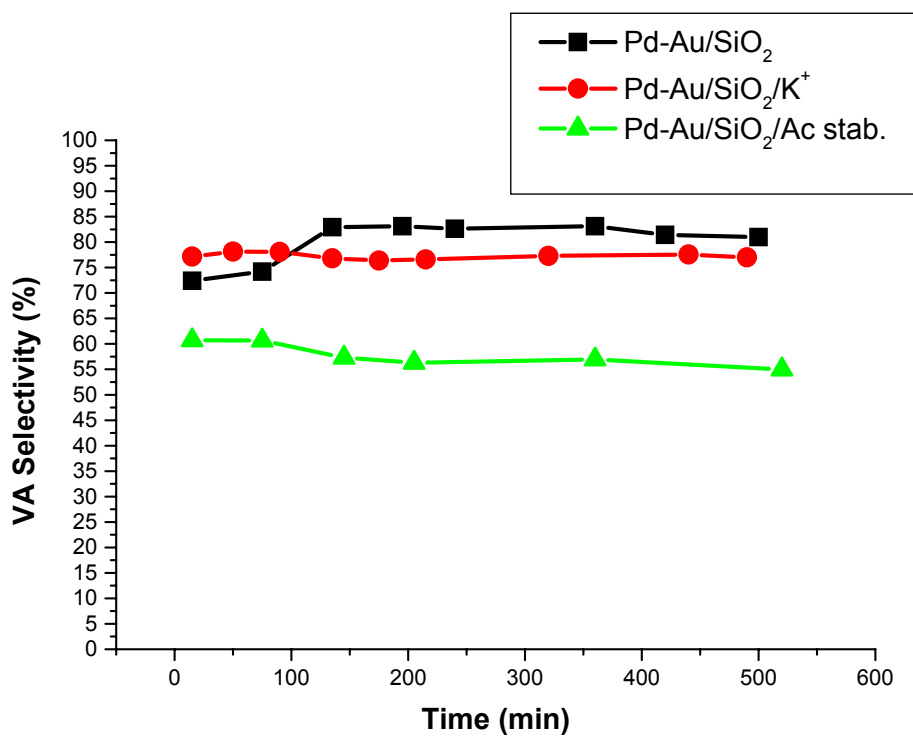
Fig. 40.   VA selectivities (▪: Pd-Au/SiO$_2$, •: Pd-Au/SiO$_2$/K$^+$, ▲: acetate-based Pd-Au/SiO$_2$) in the synthesis of vinyl acetate: feed gas, p$_{C_2H_4}$ = 7.5 kPa, p$_{O_2}$ = 1.0 kPa, p$_{AcOH}$ = 2.0 kPa, rest N$_2$; total flow rate, 60 ml/min at 423 K.

Temperature Effects

As mentioned earlier, the rate of the reaction increases with an increase in temperature, whereas the selectivity goes down. Therefore, these two indices of catalyst performance move in the opposite direction with temperature. In the present study, VA synthesis was carried out using acetate-based Pd-Au/SiO_2 under different temperatures, 130 ^{o}C, 150 ^{o}C and 170 ^{o}C. It is evident that the reaction rate of acetate-based Pd-Au/SiO_2 at 130 ^{o}C is approximately 3 times lower than the reaction rates at 150 ^{o}C and 170 ^{o}C as shown in the Fig.41. However, the reaction rate of acetate-based catalyst at 130 ^{o}C was comparable to the reaction rate of Pd-Au/SiO_2 and Pd-Au/SiO_2/K^+ catalysts. On the other hand, the selectivity of acetate-based Pd-Au/SiO_2 at 130 ^{o}C was 40% higher than the selectivities at 150 ^{o}C and 170 ^{o}C as shown in Fig. 42. The selectivity at 130 ^{o}C was observed to be 100% as is evident between 15-450 min. Therefore, the use of acetate-based Pd-Au/SiO_2 seems very promising and should be explored further.
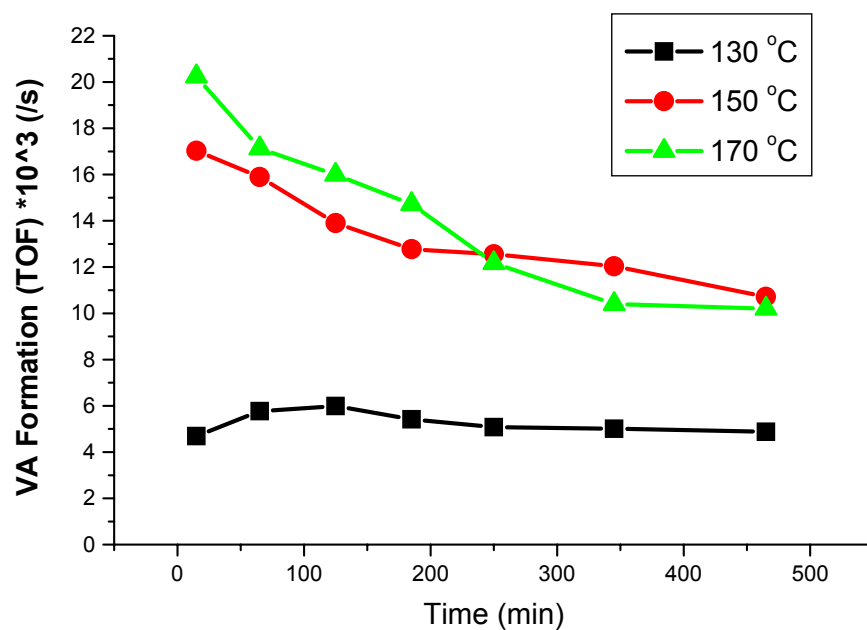
Fig. 41.   Reaction rates of acetate-based Pd-Au/SiO$_2$ catalyst as a function of temperature (■: 130 ^{o}C, •: 150 ^{o}C, ▲: 170 ^{o}C) in the synthesis of vinyl acetate: feed gas, p$_{C_2H_4}$ = 7.5 kPa, p$_{O_2}$ = 1.0 kPa, p$_{AcOH}$ = 2.0 kPa, rest N$_2$; total flow rate, 60 Nml/min at   423 K.
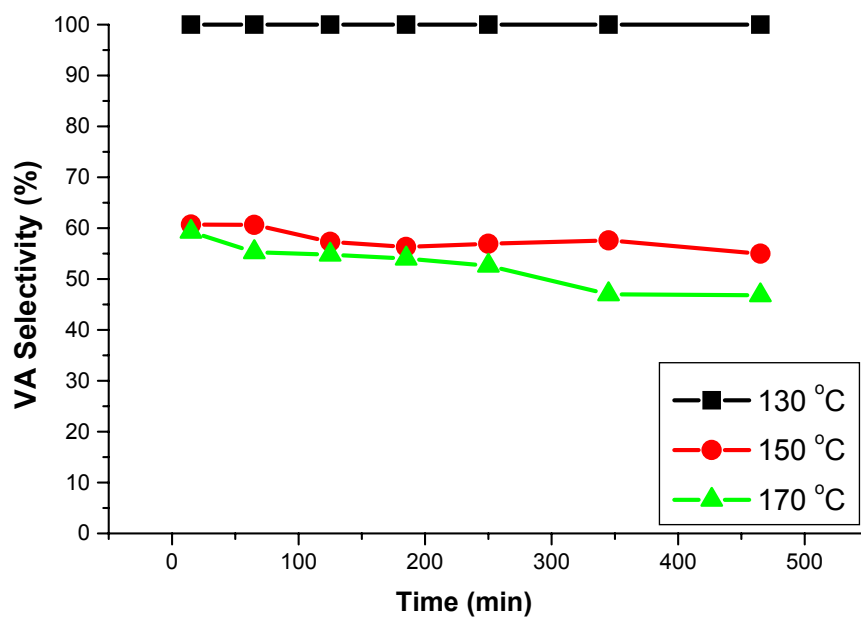
Fig. 42.   VA selectivities of acetate-based Pd-Au/SiO$_2$ catalyst as a function of temperature ($\blacksquare$: 130 ^{o}C, $\bullet$: 150 ^{o}C, $\blacktriangle$: 170 ^{o}C): feed gas, $p_{C_2H_4}$ = 7.5 kPa, p_{O_2} = 1.0 kPa, p_{AcOH} = 2.0 kPa, rest N$_2$; total flow rate, 60 N ml/min at 423 K.

CO Oxidation

In the present study, unsupported acetate-based Pd-Au catalyst and supported acetate-based Pd-Au/SiO$_2$ were used for CO oxidation studies. In the CO oxidation experiments, CO and O$_2$ (1:2) were passed over the catalyst and the temperature was increased at 15 minute intervals in increments of 10 ^{o}C until 100% CO conversion was obtained. The products were analyzed and 100% CO conversion was obtained at 160 ^{o}C for unsupported acetate-based Pd-Au catalyst. On the other hand, 100% CO conversion was obtained at 190 ^{o}C for supported acetate-based Pd-Au/SiO$_2$ catalyst as shown in Fig.43. These CO oxidation results for unsupported acetate-based Pd-Au catalyst are comparable to the results obtained using conventional Pd-Au/SiO$_2$ catalysts. These results strongly imply that oxide supports do play a significant role in the catalytic behavior of this metal. It was observed that Au catalysts on inert oxide supports need to be prepared in a highly dispersed state [4]. Also, CO is able to adsorb on small metallic gold particles compared to massive particles [4]. As mentioned, the particle size of acetate-based catalyst is 19-20 nm, which accounts for the lower CO conversion.
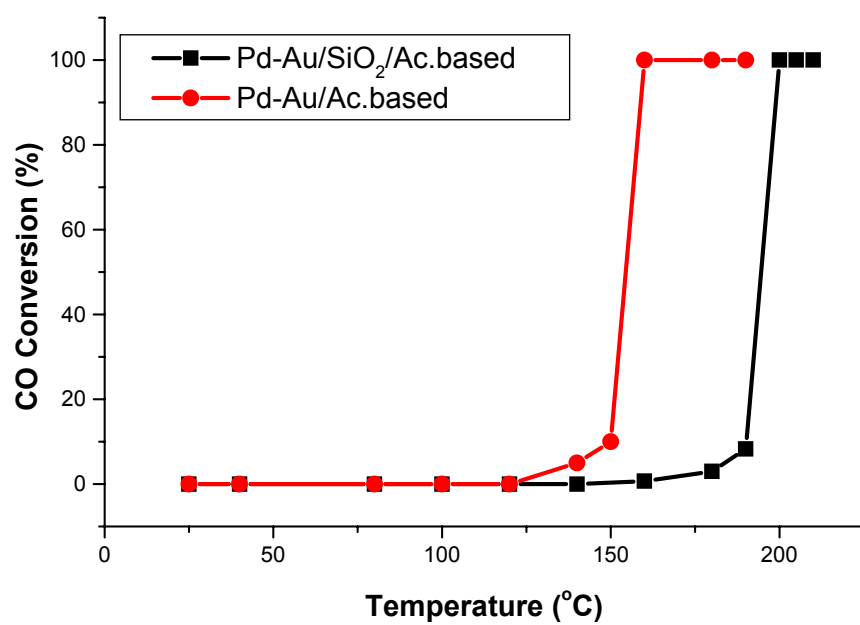
Fig. 43.   Conversion of CO as a function of temperature for acetate-based Pd-Au catalyst: feed gas, p_{CO_2} = 2 kPa, p_{O_2} = 1.0 kPa, rest N_2; catalyst sample: 50 mg.

Polymer-Based Pd-Au catalyst

Polyvinylpyrrolidone (PVP) is a white, hygroscopic powder with a weak characteristic odor. In contrast with most polymers, PVP is readily soluble both in water and in a large number of organic solvents, such as alcohol, amines, acids and chlorinated hydrocarbons [52]. On the other hand, the polymer is insoluble in common esters, ethers, hydrocarbons, and ketones. The marked hygroscopicity of PVP and adhesion to different materials are characteristic properties of PVP. This property combined with outstanding film formation, high capacity for complex formation, good stabilizing and solubilizing capacity have made PVP one of the most frequently used specialty polymers. PVP is synthesized by free-radical polymerization of N-vinylpyrolindone in water or alcohols with a suitable initiator [52]. In the present study, we synthesized polymer-based catalyst by centrifuging PVP with Pd-Au precursor solutions and silica support at room temperature.

VA Synthesis

XRD patterns were obtained for freshly reduced catalysts as shown in Fig. 44. XRD reveals two diffraction features at Bragg angles of 40.2 and 46.2^{o}, corresponding to polycrystalline Pd(111) and Pd(200) respectively. Using Eq. 19, the particle size for the catalysts was determined to be 20 nm. TEM images were obtained for this catalyst, one of which is shown in Fig. 45. Approximately 300 particles were measured to obtain the average particle-size of 19 nm, which is comparable to the results obtained from XRD. VA synthesis was carried out using polymer-based Pd-Au/SiO_2 catalyst and the

Fig. 44.   XRD data for polymer-based Pd-Au/SiO$_2$ catalyst after reduction at 673 K in 20 ml/min O$_2$ (10%)/N$_2$, 30 min, then 573 K in 20 ml/min H$_2$ for 30 min.

20 nm

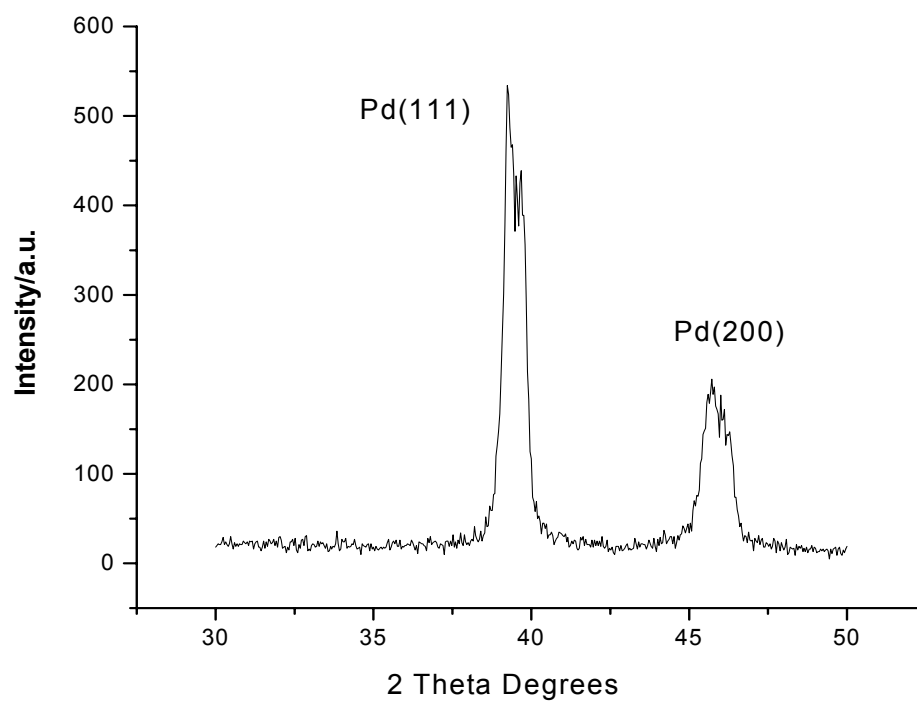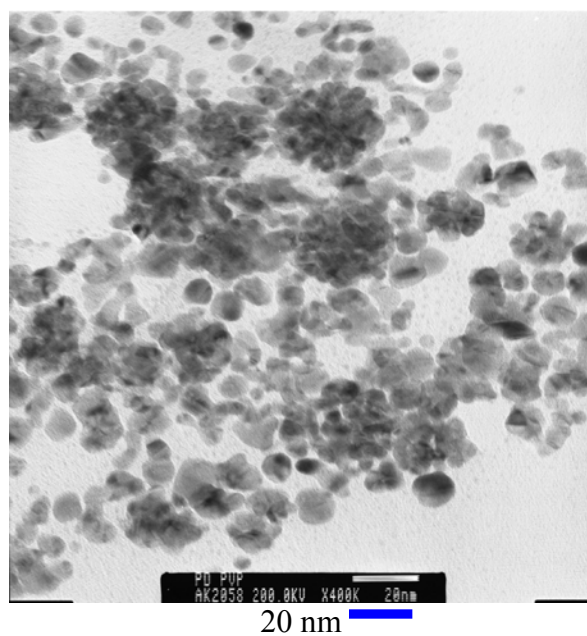Fig. 45.   TEM micrograph of polymer-based Pd-Au/SiO$_2$ catalyst after reduction at 673 K in 20 ml/min O$_2$ (10%)/N$_2$, 30 min, then 573 K in 20 ml/min H$_2$ for 30 min.
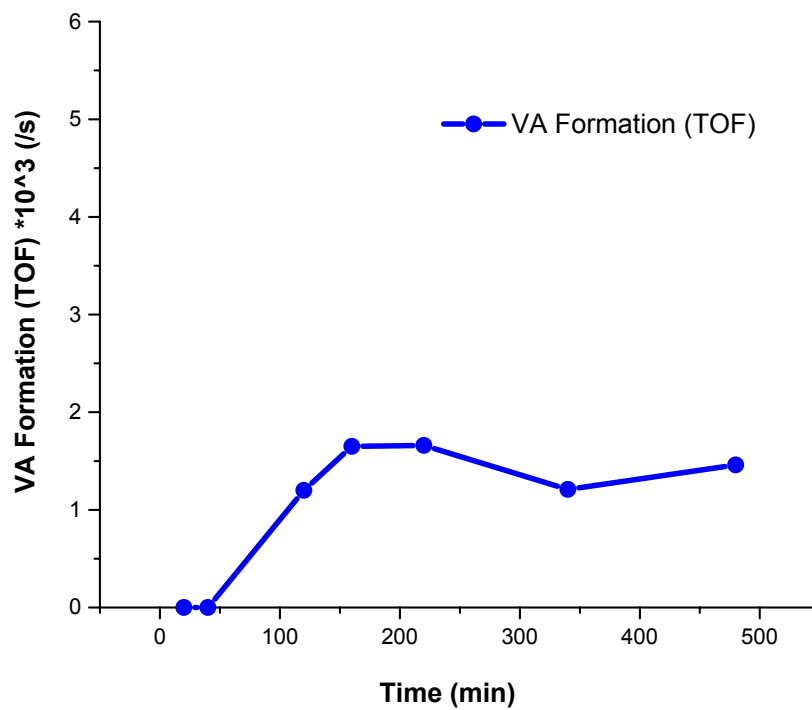
Fig. 46.   Reaction rate of polymer-based Pd-Au/SiO$_2$ catalyst in the synthesis of vinyl acetate: feed gas, pC_2H_4 = 7.5 kPa, pO_2 = 1.0 kPa, p_{AcOH} = 2.0 kPa, rest N$_2$; total flow rate, 60 Nml/min at 423 K.

corresponding VA activity was measured. From Fig. 46 it is evident that the reaction rate of polymer-based Pd-Au/SiO_2 is lower (x 6) compared to acetate-based Pd-Au/SiO_2 catalysts. Furthermore, the reaction rate is also lower than conventional Pd-Au catalysts.

CO Oxidation

In our experiment, unsupported polymer-based Pd-Au catalyst and supported polymer-based Pd-Au/SiO_2 were used for CO oxidation studies. CO and O_2 (1:2) were passed over the catalyst and the temperature increased at 15 minute intervals in increments of 10 ^{o}C until 100% CO conversion was obtained. The products were analyzed and 100% CO conversion was obtained at 160 ^{o}C for unsupported polymer-based Pd-Au catalyst. On the other hand, 100% CO conversion was obtained at 210 ^{o}C for supported polymer-based Pd-Au/SiO_2 catalyst as shown in Fig. 47. The CO conversion results using unsupported polymer-based Pd-Au/SiO_2 were also comparable to conventional Pd-Au catalysts. The CO conversion results were identical for unsupported acetate-based and polymer based catalysts. Also, CO conversion decreased for supported polymer-based Pd-Au/SiO_2 catalyst, strongly suggesting that the Pd-Au particles are likely highly dispersed.
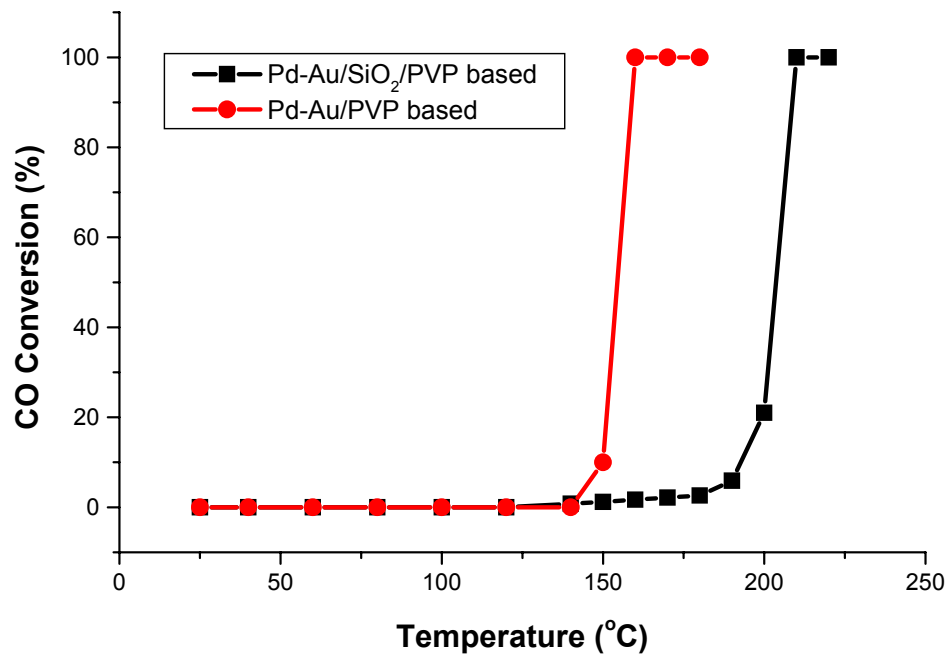
Fig. 47.   Conversion of CO as a function of temperature for supported polymer-based
Pd- Au/SiO$_2$ catalyst: feed gas, p$_{CO_2}$ = 2.0 kPa, p$_{O_2}$ = 1.0 kPa, rest N$_2$; catalyst
sample:50 mg.

SUMMARY

It is evident that the addition of Au to Pd leads to an increase in activity and selectivity. This surface modification is an important factor in the altered reaction kinetics for VA synthesis and CO oxidation reactions. Promoted and unpromoted Pd-Au/SiO_2/K^+ catalyst were used for VA synthesis and the effect of pre-adsorbed O_2, acetic acid and the role of oxygen were explored. The VA reaction rate of novel acetate-based Pd-Au/SiO_2 catalyst was 3.5 times higher than conventional Pd-Au catalysts. Also, 100% selectivity was obtained for acetate-based Pd-Au/SiO_2 at 130 ^{o}C and the VA formation rate was comparable to that of conventional Pd-Au/SiO_2 and Pd-Au/SiO_2/K^+ catalysts. Therefore, acetate-based Pd-Au/SiO_2 catalysts are very promising and should be explored further. Pd(1):Au(4)/SiO_2 catalysts demonstrate 100% CO conversion at much lower temperatures (90 ^{o}C) compared with other Pd-Au based catalysts. Furthermore, in the CO oxidation reactions, the metal loading was increased to 5 wt % in order to obtain sufficient CO oxidation activity with increased particle sizes. Finally, these catalysts did not deactivate under above-ambient reaction temperature conditions, which suggests that 1:4 Pd-Au/SiO_2 catalysts are good candidates for CO oxidation catalysts.

REFERENCES

[1] C. N. Satterfield. *Heterogeneous Catalysis in Practice*; McGraw-Hill Chemical Engineering Series, New York, 1980.

[2] M. Boudart. Principles of Heterogeneous Catalysis. In Handbook of Heterogeneous Catalysis; G. Ertl, H. Knozinger, J. Weitkamp, Eds.; VCH: Weinheim, Federal Republic of Germany, 1997; Vol. 1, 2.

[3] Y.-F. Han, D. Kumar, D.W. Goodman, J. Catal. 230 (2005) 362.

[4] A. M. Venezia, L. F. Liotta, G. Pantaleo, V. La Parola, G. Deganello, A. Beck, Zs. Koppány, K. Frey, D. Horváth, L. Guczi, Appl. Catal., A:General 251 (2003) 359.

[5] K. Gossner, E. Mizera, J. Electroanal. Chem. 98 37 (1979).

[6] Y.-F. Han, J.-H. Wang, D. Kumar, Z. Yan, D.W. Goodman, J. Catal. 232 (2005) 473.

[7] C.-W. Yi, K. Luo, T. Wei, D.W. Goodman, J. Phys. Chem, B (accepted) 2006.

[8] Y.-F. Han, D. Kumar, C. Sivadinarayana, A. Clearfield, D.W. Goodman, Catal. Lett. 94 (2004) 131.

[9] M. Haruta, Catal. Today 36 (1997) 153.

[10] A. M. Venezia, V. La Parola, N. Nicoli, G. Deganello, J. Catal. 212 (2002) 56.

[11] C.J. Baddeley, M. Tikhor, C. Hardacre, J.R. Lomas, R.M. Lambert, J. Phys. Chem. 100 (1996) 2189.

[12] M.S. Chen, K. Luo, T. Wei, D. Kumar, C.W. Yi, D.W. Goodman, Catal. Today (accepted) 2006.

[13] A. Jablonski, S.H. Overbury, G.A. Somorjai, Surf. Sci. 65 (1977) 578.

[14] B.J. Wood, H. Wise, Surf. Sci. 52 (1975) 151.

[15] A. M. Venezia, V. La Parola, B. Pawelec, J. L. G. Fierro, Appl. Catal. A 264 (2004) 43.

[16] I.I. Moiseev, M.N. Vargaftik, Y.K. Syrkin, Dokl. Akad. SSSR 133 (1960) 377.

[17] T. Kawaguchi, T. Wakasugi, App. Catal. 36 (1988) 67.
[18] M. EL- Sawi, G. Emig, H. Hofman, Chem. Engg. Journal 13 (1977) 201.

[19] S. Nakamura, T. Yasui, J. Catal. 17 (1970) 366.

[20] M. Neurock, W.D. Provine, D.A. Dixon, G.W. Coulston, J.J. Lerou, R.A. Vansanten, Chem. Eng. Sci. 51 (1996) 1691.

[21] M. Neurock, J. Catal. 216 (2003) 73.

[22] M. Neurock, D. Mei, Top. Catal. 20 (2002) 5.

[23] K. Luo, T. Wei, C.-W. Yi, S. Axnanda, D.W. Goodman, J. Phys. Chem. B 109 (2005) 23517.

[24] B. Samanos, P. Boutry, R. Montarnal, J. Catal. 23 (1971) 19.

[25] S. A. H. Zaidi, Appl. Catal. 38 (1988) 353.

[26] W. D. Provine, P. L. Mills, J. J. Lerou, Stud. Surf. Sci. Catal. 101 (1996) 191.

[27] M.S. Chen, D. Kumar, C.W. Yi, D.W. Goodman, Science 310 (2005) 291.

[28] M. Date, Y. Ichihashi, T. Yamashita, A. Chiorino, F. Boccuzzi, M. Haruta, Catal.Today 72 (2002) 89.

[29] T. F. Jaramillo, S.H. Baeck, B.R. Cuenya, E.W. McFarland, J. Am. Chem. Soc. 125 (2003) 7148.

[30] L.M. Molina, B. Hammer, Phys. Rev. Lett. 90 (2003) 20.

[31] J. M.C. Soares, P. Morrall, A. Crossley, P. Harris, M. Bowker, J. Catal. 219 (2003) 17.

[32] M. Valden, X. Lai, D.W. Goodman, Science 281 (1998) 1648.

[33] M.S. Chen, D.W. Goodman, Science 306 (2004) 253.

[34] Y. Iizuka, H. Fujiki, M. Haruta, Catal. Today 36 (1997) 115.

[35] S. Nakamura, T. Yasui, J. Catal. 23 (1971) 315.

[36] T.V. Choudhary, D.W. Goodman, Top. Catal. 21 (2002) 32.

[37] A. Bourane, D. Bianchi, J. Catal. 220 (2003) 3.

[38] B.T. Charles, US Patent 4,048,096 (1997).

[39] SRI Instruments, GC Detectors,
http://www.srigc.com/2005catalog/cat46.html, 2006.

[40] Library 4 Science, Gas Chromatography,
www.chromatography-online.org/GC/Detectors/Flame-Ionization/rs38.html, 2006.

[41] N. Macleod, J. Keel, R.M. Lambert, App. Catal. A: General 261(2004) 37.

[42] Y.-F. Han, D. Kumar, C. Sivadinarayana, D.W. Goodman, J. Catal. 224 (2004) 60.

[43] W.D. Provine, P.L. Mills, J.J. Lerou, Stud. Surf. Sci. Catal. 101 (1996) 191.

[44] K. Gossner, E. Mizera, J. Electroanal. Chem. 98 37 (1979).

[45] E.M. Stuve, R.J. Madix, Surf. Sci. 160 (1985) 293.

[46] D.Stacchiola, M.Neurock, T.Tysoe, Angew. Chem. 44 (2005) 4572.

[47] E.A. Crathorne, D. MacGowan, S.R. Morris, A.P. Rawlinson, J. Catal. 149 (1994) 254.

[48] M. Bowker, C. Morgan, J. Couves, Surf. Sci. 555 (2004) 146.

[49] D. Stacchiola, M. Neurock, T.Tysoe, J. Am. Chem. Soc. 126 (2004) 15384.

[50] D. Kumar, Y.-F. Han and D.W. Goodman, Catal. Lett. (accepted) 2006.

[51] S. Shaikhutdinov, M. Heemeier, M. Baumer, T. Lear, H.-J. Freund, J. Catal. 200 (2001) 330.

[52] BASF Corporation, Functional Polymers,
www.basf.com/businesses/consumer/dispersions/usa/pvp/index.html, 2006.

VITA

Praveenkumar Boopalachandran was born in Tamilnadu, India. He received a "B.Tech." degree in Chemical Engineering from the University of Madras, India in July 1999. In January 2002, he received his Master of Science degree (General Chemistry) from Texas A&M University, Commerce. He held responsible positions such as president for the International Student Association (AIS) and a senator in the Student Government Association (SGA). In August 2003, Praveenkumar enrolled in graduate school in the Department of Chemistry of Texas A&M University, College Station under the guidance of Dr. D. Wayne Goodman. He was a mentor instructor assistant (head of lab instructors) for Chemistry 102 laboratory. Praveenkumar was awarded his Master of Science degree (Physical Chemistry) in May 2006.

Permanent address: No: 11 Perumal Koil street,
　　　　　　　　　Kottur,
　　　　　　　　　Chennai 6000 85, India